CONTRACT NO. A932-113
FINAL REPORT
JUNE 1993

Investigation of the Effects of Atmospheric Acidity Upon Economically Significant Materials

CALIFORNIA ENVIRONMENTAL PROTECTION AGENCY

AIR RESOURCES BOARD
Research Division

INVESTIGATION OF THE EFFECTS OF ATMOSPHERIC ACIDITY UPON ECONOMICALLY SIGNIFICANT MATERIALS

Final Report
Contract No. A932-113

Prepared for:

California Air Resources Board
Research Division
2020 L Street
Sacramento, California 95814

Submitted by:

University of Southern California
Los Angeles, CA 90089-02531

Prepared by:

F. Mansfeld
and
R.C. Henry

JUNE 1993

ABSTRACT

A number of materials of economic significance have been exposed at three sites in Southern California (Burbank, Long Beach and Upland) and at a background site in Central California (Salinas) during the time between March 1986 and August 1990. These materials were galvanized steel, nickel, aluminum, two types of flat latex exterior house paint, nylon fabric, polyethylene and concrete. Due to experimental problems with the concrete blocks and difficulties in determining corrosion damage for polyethylene, no experimental corrosion data are available for these two materials. Corrosion damage was determined by weight loss for galvanized steel, nickel, aluminum and the two paints. For the nylon fabric the loss of breaking strength was used as a measure of corrosion damage. Atmospheric data were provided by the California Air Resources Board's air monitoring network at the test sites. Relative humidity data were obtained from local airports.

Corrosion rates were very low at all four locations. For galvanized steel the average corrosion rate was less than 1 μm/year. Such low values are usually observed only for clean, rural areas. Another interesting result is the time dependence of corrosion rates. For galvanized steel, nickel, and aluminum, corrosion rates were higher in the summer than in the winter, which is opposite to the time dependence observed at most other locations worldwide. It is very likely that the time dependence observed in Southern California is due to photochemically produced acids, particularly nitric acid (HNO_3), for which concentrations peak during the summer months. However, this conjecture could not be proven because reliable, long term HNO_3 monitoring data were not available for the four test sites during the study.

A multivariate regression analysis of the experimental corrosion and aerometric data showed that the observed corrosion damage could be explained satisfactorily for galvanized steel, nickel, and aluminum using variables related to O_3 concentrations and relative humidity. O_3 itself is not corrosive, but it is a good indicator of photochemically produced HNO_3 and perhaps other components of smog that are direct causes of corrosion. Based on the regression equations estimates can be made concerning the reduction of corrosion damage due to the reduction of acidic deposition in California. However, because the relationship of O_3 to the underlying, direct agents of corrosion is site-specific, the results are valid only for the monitoring sites included in this study and cannot be applied to estimate the cost of materials damage in the South Coast Air Basin or statewide.

DISCLAIMER

"The statements and conclusions in this report are those of the contractor and not necessarily those of the California Air Resources Board. The mention of commercial products, their source or their use in connection with material reported herein is not to be construed as either an actual or implied endorsement of such products."

ACKNOWLEDGEMENTS

The air quality data were collected and processed by Mr. Kadio Ahossane, Ph.D. candidate in the Environmental Engineering Program at the University of Southern California.

The relative humidity data were collected and processed by Mr. William Moran, Ph.D. candidate in the Environmental Engineering Program at the University of Southern California.

The corrosion damage data were collected and processed by Mr. Hong Xiao, Ph.D. candidate in the Department of Materials Science and Engineering at USC.

Table of Contents

List of Figures

List of Tables

1 Introduction

The Kapiloff Acid Deposition Act of 1982 (California Health and Safety Code, Sections 39010.5, 39010.6, 39900 et seq.) required the California Air Resources Board (CARB) to assess the economic impact of acid deposition upon materials as part of a comprehensive research program to determine the nature, extent, and potential effects of acid deposition in California. To this end, the CARB contracted with the Environmental Monitoring and Services (EMSI) group of Combustion Engineering Inc. (now ABB, Inc.) and the Department of Materials Science of the University of Southern California (USC). Field exposures were conducted by EMSI, and USC carried out a series of laboratory studies. The main purpose of these studies was to determine damage functions that could then be used in an economic analysis of the costs of materials damage by acid deposition in California. These studies (CARB contracts A4-110-32 and A5-137-32) were concluded in 1988 (1). The same investigators also carried out a study (CARB contract A5-138-32) to determine the role of acid fog on materials in California (2).

At the end of the above studies, the exposure racks were left at the sites with some coupons (small, rectangular samples of materials) exposed. In the summer of 1991, CARB contracted with USC to remove the racks from the sites, collect the remaining coupons, make damage measurements, and analyze the total data set

collected during the field studies (not including the acid fog study).

This report summarizes this last, and final, stage of this multi-year project. A brief review of the experimental procedures is given in this report. However, details such as the quality assurance and control protocol are described in a previous report (1). Next, the results of all the ambient exposures for the entire project are presented and discussed. Finally, the multivariate statistical analysis used to estimate the relationships between corrosion rates, air quality, and meteorological parameters is discussed and the results are described.

2 Experimental Approach

The experimental approach used in this project has been described in great detail in the final report (1) for two previous CARB projects (A4-110-32 and A5-137-32). The previous report also discusses the rationale for the selection of the materials and the test sites, and contains a description of the methods for determination of damage after exposure. The most important features of the experimental approach are summarized in this report.

Sample preparation and exposure procedures and methods of damage assessment were based on the following guidelines: ASTM G50, "Standard Practice for Conducting Atmospheric Corrosion Tests on Metals"; ASTM G1, "Standard Practice for Preparing, Cleaning and Evaluating Corrosion Test Specimens"; ASTM D1682, "Breaking Load and Elongation of Textile Fabrics"; and specific material procedures developed in U. S. Environmental Protection Agency (EPA) programs. Where required, these procedures were modified or additional standard operating procedures were developed (1).

2.1 Materials

The choice of the materials exposed in this study was based primarily on the potential economic consequences of damage to materials susceptible to degradation due to acid deposition. The

materials were chosen based on the extent of usage, susceptibility to damage due to acid precipitation, costs of materials, maintenance, repair, and replacement costs (3). Considerations also included limitations due to available field exposure times, sample size and methods of damage assessment. The final selection of materials was made by joint agreement between CARB personnel and the project participants. The following materials were exposed:

1. zinc (Zn as galvanized steel)
2. nickel (Ni)
3. flat latex exterior house paint with carbonate extender (on stainless steel) (H-C)
4. flat latex exterior house paint without carbonate extender (on stainless steel) (L-C)
5. concrete (as commercial concrete bricks)
6. aluminum (Al)
7. nylon fabric (Fabric)
8. polyethylene plastic
9. flat latex exterior house paint without carbonate extender (on wood)

The first five materials were first exposed in February and March 1986, the remaining four materials were added in July 1987 (Table 2-1).

Preparation of Materials for Exposure Tests

The metallic materials (galvanized steel, nickel, aluminum and the stainless steel serving as the substrate for the paint) were sheared to 15.2 cm x 10.2 cm (6 inch x 4 inch) and deburred to remove sharp edges. Holes for identification of individual samples were punched followed by degreasing to remove grease, fingerprint and ink marks. The samples were given a final rinse with deionized water, dried, equilibrated for 24 hours and then weighed. The samples were then placed in individual bags and stored in light excluding cardboard boxes. The following are the properties of the materials used for the exposure tests:

Nickel - nickel 200 (chemically pure), 24 gauge.

Galvanized steel - electro-galvanized, non-chromated steel, 24 gauge.

Aluminum - Al 1100 H-14, 0.051 cm thick (0.02 inch).

Stainless steel - type 304, 24 gauge, lightly sanded and acid washed before painting.

Polyethylene - high density polyethylene, 0.32 cm (1/8 inch) sheet thickness. Samples were wiped with Kimwipes, washed in mild detergent, rinsed in deionized water and dried.

Nylon fabric - nylon cloth used for the outer shell of garments and tents (Glen Raven Mills, Inc.). The preparation procedure for the nylon fabric was developed in consultation with Dr. Christine Ladisch of the Purdue University Textile Laboratory and is described in the previous report (1).

Paints - vinyl acrylic interior-exterior Navajo white house paint from two different manufacturers ("high" and

"low" carbonate paint). Paint was applied to stainless steel by spray painting with thin multiple coats for a total paint thickness of about 1.3 mm.

Wood - the low-carbonate paint was also applied to wood (Western Red Cedar). The special properties of wood as a substrate for paint made it necessary to develop special procedures for pretreatment and painting, which were established in consultation with R. Sam Williams at the USDA Forest Service, Forest Products Laboratory (1).

Concrete - concrete samples were cut to 3.8 cm x 3.8 cm x 10.2 cm (1.5 inch x 1.5 inch x 4 inch) blocks from concrete building bricks.

As will be discussed below, no meaningful damage data could be obtained for the polyethylene, paint on wood and concrete samples. The detailed procedures for sample preparation and damage analysis, which can be found in the previous report (1), are therefore not repeated here for these materials.

2.2 Exposure Conditions and Test Sites

Four tests sites were selected for this project, three of which are located in the South Coast Air Basin (Burbank -BR, Long Beach -LB and Upland -UP), while the fourth (Salinas -SL in Central California) serves as a relatively unpolluted background site. The annual average SO_2 concentration for Salinas has been reported as 0.2 ppb, while for the three test sites in Southern California values between 2.1 ppb (Upland) and 9.8 ppb (Long Beach) have been reported (1).

Duplicate samples for each exposure period were mounted per ASTM G50 on exposure racks inclined at 30° to the horizontal and facing south. The samples were held in place by porcelain insulators in order to avoid galvanic corrosion between the samples and the rack material (galvanized steel). For the concrete and the nylon fabric samples, somewhat different mounting procedures were used (1). All materials were at least 1.2 m above the ground. All test racks were situated above gray-white crushed-rock-covered roofing paper or gravel-covered ground.

In order to determine seasonal effects on atmospheric corrosion rates, it was initially planned to use three-month and six-month exposure periods in addition to longer term periods. Quarterly (three-month) samples are desirable for the statistical analysis of the correlation between atmospheric parameters and corrosion damage. However due to budgetary restraints, it was only possible to use quarterly samples during the first year of this project. Samples first exposed in December 1987 and later remained exposed for periods of nine months or longer. Table 2-1 lists the dates at which samples were first exposed. Eight sets of galvanized steel (Zn), nickel (Ni) and paint on stainless steel (H-C for "high" carbonate, L-C for "low" carbonate paint) were first exposed between February 1986 and September 1989. Four sets of aluminum (Al) and nylon fabric (Fabric) were exposed beginning between July 1987 and September 1989. Concrete,

polyethylene and paint on wood are not listed in Table 2-1, since no meaningful damage data could be obtained for these samples.

2.3 Damage Measurements

The degree of damage after a given exposure period was determined by weight loss measurements for the metals and the paint on stainless steel and by strength loss for the nylon fabric. Since the stainless steel substrate can be assumed to experience no weight change, the measured weight loss can be attributed to the weight loss of the paint. For Al, weight loss data are only available for samples collected after October 1987. No meaningful damage data could be obtained for the paint on wood, polyethylene and concrete samples. For the paint on wood, appearance measurements were the primary damage measurements. However, as discussed previously (1), this analysis was complicated by poor sample conditions (cracking and breaking of the wood) after the test. While it was possible to detect damage to paint color, it was not possible to differentiate between damage at different test sites or seasons (1). Various surface analysis methods were considered for the polyethylene samples, however no simple, inexpensive method could be identified. For the concrete samples, a weight gain was determined in most cases. However, due to problems caused by breaking of the samples and other uncertainties in the damage measurements, concrete samples were not included in the final damage analysis.

The weight loss, W, is determined as the difference of the weight of the unexposed sample w(0) and the weight after exposure w(t) for a time period t corrected for the weight loss, w_b, of an unexposed sample in the descaling solution which is used for the removal of corrosion products:

$$W = w(0) - w(t) + w_b \qquad (1).$$

All samples were first photographed when they were returned from field exposure. They were then rinsed in deionized water and immersed in a descaling solution which was material specific. Finally the samples were rinsed, dried, equilibrated and weighed. A detailed account of these procedures is given in the previous report (1). The following gives a brief summary of the descaling procedure for each material. The test procedure for nylon fabric is also described briefly.

Galvanized steel - immersion in saturated ammonium acetate at room temperature for 2 hours.

Nickel - immersion in deaerated hydrochloric acid (HCl) for 90 seconds per ASTM G1.

Aluminum - immersion in a solution of chromic and phosphoric acid at 90°C for 7 minutes.

Paint on stainless steel - washing in a solution of a mild

nonionic surfactant followed by a rinse in deionized water, drying at 70°C for one hour and equilibration in the weighing room for 24 hours before weighing.

Nylon Fabric - measurement of the breaking strength of exposed and unexposed (blank) samples was carried out with an Instron Universal Testing Instrument model 1130 according to ASTM D1682. All samples were conditioned at 21°C and RH = 65% for at least 48 hours before testing. A minimum of five warpwise raveled strips from each sample was tested (1).

Table 2-1 Dates of First Exposure at the Four Test Sites

sets		Zn	Ni	H-C	L-C	Al	Fabric
BR	1st	Feb. 27,'86	Feb. 27,'86	Mar. 12,'86	Mar. 12,'86		
	2nd	Jun. 24,'86	Jun. 24,'86	Jun. 24,'86	Jun. 24,'86		
	3rd	Oct. 4,'86	Oct. 4,'86	Oct. 4,'86	Oct. 4,'86		
	4th	Jan. 22,'87	Jan. 3,'87	Jan. 3,'87	Jan. 3,'87		
	5th	Jul. 8,'87	Jul. 8,'87	Jul. 8,'87	Jul. 8,'87	Jul. 8,'87	Jul. 8,'87
	6th	Oct. 5,'87	Oct. 5,'87	Oct. 5,'87	Oct. 5,'87	Oct. 5,'87	Oct. 7,'87
	7th	Jan. 8,'88	Jan. 8,'88	Jan. 8,'88	Jan. 8,'88	Jan. 8,'88	Jan. 8,'88
	8th	Sep. 27,'89	Sep. 27,'89	Sep. 27,'89	Sep. 27,'89	Sep. 27,'89	Sep. 27'89
LB	1st	Mar. 3,'86	Mar. 3,'86	Mar. 3,'86	Mar. 3,'86		
	2nd	Jun, 24,'86	Jun. 24,'86	Jun. 24,'86	Jun. 24,'86		
	3rd	Oct. 3,'86	Oct. 3,'86	Oct. 3,'86	Oct. 3,'86		
	4th	Jan. 22,'87	Jan. 2,'87	Jan. 2,'87	Jan. 2,'87		
	5th	Jul. 7,'87	Jul. 7,'87	Jul. 7,'87	Jul. 7,'87	Jul. 7,'87	Jul. 10,'87
	6th	Oct. 2,'87	Oct. 2,'87	Oct. 2,'87	Oct. 2,'87	Oct. 2,'87	Oct. 2,'87
	7th	Jan. 22,'88	Jan. 22,'88	Jan. 22,'88	Jan. 22,'88	Jan. 22,'88	Jan. 22,'88
	8th	Sep. 26,'89	Sep. 26,'89	Sep. 26,'89	Sep. 26,'89	Sep. 26,'89	Sep. 26,'89
SL	1st	Mar. 27,'86	Mar. 27,'86	Mar. 27,'86	Mar. 27,'86		
	2nd	Jun. 26,'86	Jun. 26,'86	Jun. 26,'86	Jun. 26,'86		
	3rd	Oct. 1,'86	Oct. 1,'86	Oct. 1,'86	Oct. 1,'86		
	4th	Jan. 23,'87	Jan. 23,'87	Jan. 23,'87	Jan. 23,'87		
	5th	Jul. 23,'87	Jul. 23,'87	Jul. 23,'87	Jul. 23,'87	Jul. 23,'87	Jul. 23,'87
	6th	Dec. 4,'87	Dec. 4,'87	Dec. 4,'87	Dec. 4,'87	Dec. 4,'87	Dec. 4,'87
	7th	Feb. 5,'88	Feb. 5,'88	Feb. 5,'88	Feb. 5,'88	Feb. 5,'88	Feb. 5,'88
	8th	Oct. 3,'89	Oct. 3,'89	Oct. 3,'89	Oct. 3,'89	Oct. 3,'89	Oct. 3,'89
UP	1st	Mar. 14,'86	Mar. 14,'86	Mar. 14,'86	Mar. 14,'86		
	2nd	Jun. 24,'86	Jun. 24,'86	Jun. 24,'86	Jun. 24,'86		
	3rd	Oct. 3,'86	Oct. 3,'87	Oct. 3,'86	Oct. 3,'86		
	4th	Jan. 22,'87	Jan. 2,'87	Jan. 2,'87	Jan. 2,'87		
	5th	Jul. 8,'87	Jul. 8,'87	Jul. 8,'87	Jul. 15,'87	Jul. 8,'87	Jul. 15,'87
	6th	Oct. 7,'87	Oct. 7,'87	Oct. 7,'87	Oct. 7,'87	Oct. 7,'87	Oct. 7,'87
	7th	Feb. 14,'88	Feb. 14,'88	Feb. 14,'88	Feb. 14,'88	Feb. 14,'88	Feb. 14,'88
	8th	Sep. 29,'89	Sep. 29,'89	Sep. 29,'89	Sep. 29,'89	Sep. 29,'89	Sep. 29,'89

BR--Burbank; LB--Long Beach; SL--Salinas; UP--Upland

3 Experimental Results and Discussion

In the following, the damage data and the air quality data for the period between the first exposure in February 1986 and the removal of the last samples in August 1990 will be discussed.

3.1 Damage Data

The experimental weight loss data have been inspected by plotting the weight loss (or loss of breaking strength for nylon) as a function of exposure time at the four sites - Burbank (BR), Long Beach (LB), Upland (UP) and Salinas (SL). Table 2-1 lists the start dates for exposure of the eight sets of samples of galvanized steel (Zn), nickel (Ni), "low-carbonate" paint (L-C), "high-carbonate" paint (H-C), the four sets of aluminum (Al) and the two sets of nylon fabric (Fabric) for which damage data are available up to July 1988. The nylon samples which were collected in the summer of 1990 could not be analyzed due to excessive degradation or total destruction.

In the following, the results obtained for all sets of a given material will be shown for Burbank. In addition, the results for the first set of a material will be plotted for all four sites. A survey of the experimental data for all test sites and sets of material will be presented as plots of log W (weight loss) vs log t (exposure time).

The precision of the weight loss measurements which are plotted in Figures 3-1 to 3-15 are given in Table 3-1. Since the materials were exposed in paired samples, the precision was determined by calculating the standard deviation of difference between the weight losses of the paired samples. The results vary from 3.6 mg for Al to 12.3 mg for Zn. The table gives the two sigma error bars calculated as plus or minus two times the standard deviation. Except for Al, the error bars are about ± 20 mg, or about twice the size of a plotting symbol in Figures 3-1 to 3-15. These numbers reflect more than just weighing errors; preparation, handling, and sampling errors are included as well. Thus, the error bars in Table 3-1 are a good estimate of the overall precision of the weight loss measurements.

Galvanized Steel

Figure 3-1 is an example of weight loss data obtained for all sets of a given material at a given test site as a function of exposure time. The data in Figure 3-1 are those for the eight sets of galvanized steel samples exposed at Burbank. Five of the samples, which had previously been analyzed at EMSI/ABB and for which a weight gain instead of a weight loss had been determined (1), were descaled again at USC. For two samples a weight loss was observed after the second treatment in concentrated ammonium acetate. For the other three - one sample exposed at BR between 10/86 and 1/87 and two samples exposed at UP from 10/87 to 4/88 -

a small weight gain remained. These three samples were therefore excluded from the statistical analysis discussed below.

The most significant result is the almost zero value of corrosion rates in the winter for the time period starting in October/November and ending in February/March. This observation is contrary to the results obtained in other parts of the world, where corrosion rates are usually higher in the winter due to the increased SO_2 levels. In the Final Report for the previous contract (1), the higher corrosion rates observed in Southern California in the summer were attributed to the higher levels of HNO_3. An explanation of the close to zero corrosion rates in the winter is difficult. Rain in the South Coast Air basin is not very acidic (pH about 5) and can be considered to have a cleaning action which would reduce corrosion rates observed in the rainy season between November and March. However, other factors must be involved in producing this quite unusual phenomenon. For galvanized steel and nickel, average corrosion rates are lower than 1 μm/year, which characterizes the atmosphere in the South Coast Basin as rural according to the ASTM classification.

Figure 3-2 is a graph of the weight loss data for the first set of galvanized steel which was exposed at the four test sites in February and March 1986 (Table 2-1). Very low corrosion rates were observed in the fall and winter periods of the first year (Fig. 3-2). For the maximum exposure period of 4.5 years, the largest total corrosion loss was observed at Long Beach followed by Burbank and then Upland. The smallest corrosion loss was observed at Salinas which serves as background site.

In order to estimate the time dependence of corrosion rates and at the same time survey the quality of the entire data set, the weight loss data were also plotted as log W vs log t. This type of data display is common in studies of atmospheric corrosion (4), where it is assumed that the weight loss (W) depends on the exposure time (t) in the form:

$$W = a\ t^{b}. \qquad (2a)$$

From Equation 2a the corrosion rate r_{corr} can be calculated as:

$$r_{corr} = (1/A)\ (dW/dt) = (ab/A)\ t^{b-1}, \qquad (2b)$$

where A is the sample area.

In Equation 2, "a" is a characteristic parameter for the corrosivity of the test site for a certain material and "b" is a parameter which depends on the corrosion mechanism (4,5). If

diffusion of a corrosive species is the rate determining step, b = 0.5, for a charge transfer controlled process, b = 1.0 (4). A classification of different test sites based on their corrosivity for a given material can be made based on the experimental values of the parameter a, which is defined as the weight loss after one year (Eq. 2a) or the corrosion rate (in g/m^2-year) for the first year.

Plots of log W vs log t according to Equation 2a are shown in Figure 3-3a for all eight sets of galvanized steel at Burbank. Most data points fall along the straight line, which was determined by statistical analysis. The two data points with very low weight loss during the winter periods were excluded from the analysis. These very low weight loss data points correspond to the third set which was exposed between October 1986 and January 1987 and the sixth set which was exposed between October 1987 and January 1988. The slope of the straight line in Figure 3-3a is 0.744, which suggests mixed diffusion and charge transfer control. Agreement with Eq. 2 was also observed for galvanized steel at Salinas (Figure 3-3b), Long Beach (Figure 3-3c) and Upland (Figure 3-3d) with b ranging from 0.58 at Salinas to 0.95 at Upland (Table 3-2). This result suggests a gradual change from diffusion control due to the presence of protective corrosion product layers at the background site to charge transfer control at more corrosive test sites on surfaces which were either bare or were not covered with layers which reduced diffusion of

corrosive species to the metal surface. A certain compensation effect can be observed in Figure 3-3a through 3-3c, which leads to similar corrosion rates after about one year for cases where low values of the slope b are accompanied by high values of the value a and vice versa.

Nickel

The results obtained for the weight loss of nickel are shown in Figures 3-4 through 3-6. The plots for all eight sets at Burbank (Figure 3-4) are very similar to those for galvanized steel in Figure 3-1 with close to zero corrosion rates in the winters of 1986 and 1987 (sets 3 and 6). This unusual behavior is also detected in Figure 3-5 for first set of nickel at the four test sites. After exposure for 4.5 years, corrosion losses were the highest at Burbank and Long Beach followed by Upland and Salinas for which the lowest corrosion rates were observed. In the log W vs log t plots in Figure 3-6 slopes exceeding 0.9 were determined for Upland, Long Beach and Salinas, while the slope for Burbank was b = 0.744 (Table 3-2).

Aluminum

Fewer data points are available for Al (Figures 3-7 through 3-9), which makes the analysis of the log W vs log t plots (Figure 3-9) more difficult. However, close to zero corrosion rates in the

winter of the first year of exposure are obvious in Figure 3-7 and 3-8. Due to the availability of fewer data points, the analysis of the weight loss data for Al and the resulting values of a and b in Table 3-2 are less reliable.

Paint on Stainless Steel

The two paints on stainless steel show a corrosion behavior which is quite similar to that observed for the metals insofar as most weight loss data points fall on a straight line in the log W vs log t plots. For the L-C paint some evidence can be found from an inspection of Figure 3-10 and 3-11 that corrosion rates were close to zero in the winter months of 1986 and 1987. At the end of the test, the weight loss for the samples, which had been exposed for 4.5 years, was about the same at Burbank, Long Beach and Upland, but much less at the background site in Salinas (Figure 3-11). The slopes of the log W vs log t lines for the L-C paint are between 0.5 and 0.8, indicating that diffusion of corrosive species plays a larger role for the paints than for the metals (Figure 3-12 a-d). For the H-C paint on stainless steel, a decrease of corrosion rates was also observed in the winter (Figure 3-13 and 3-14). The weight loss for the first set at the end of the final exposure period decreased in the order Long Beach > Burbank > Upland > Salinas. In general, the weight loss for the H-C paint was higher than that for the L-C paint. The dependence of weight loss of H-C paint on time is similar to that

for the L-C paint, indicating a mixed diffusion/charge transfer controlled corrosion process (Figure 3-15).

Summary

A survey of the log W vs log t plots for galvanized steel, nickel and the two paints on stainless steel shows that the data usually fall close to the straight line based on Equation 2a and can therefore be considered to be quite reliable. The data for Al, for which fewer data points are available, show more scatter. Very low corrosion rates were observed for the Al samples of the third and the sixth sets exposed at Burbank, Long Beach and Upland. Table 3-2 gives a summary of the a and b values for all materials exposed in this program. In Table 3-2, a is defined as the weight loss after one year, according to Equation 2a. The highest values of a for galvanized steel, Al and H-C paint were observed at Long Beach. For Ni and L-C paint a had the highest values at Burbank and Long Beach. Care must be taken in the interpretation of the data in Table 3-2, since apparently a compensation effect occurs with low values of the slope b coinciding with high values of a as mentioned above. This result makes extrapolation of the experimental data to exposure times longer than 4.5 years difficult.

An interesting result of this study is the fact that the loss of

breaking strength of nylon fabrics follows very similar trends as the weight loss for the other samples. Figure 3-16 summarizes all results obtained for the two sets at the four sites. The very low rates of degradation observed for the metals and the house paints during the fall and winter can also be seen in Figure 3-16 for the nylon fabric between November 1987 and April 1988. It should be noted that this effect is clearly evident for the nylon samples of the first set exposed at Salinas, where apparently no further loss of strength occurred during this time. On the other hand, for exposure at Long Beach, the loss of strength increased from 40% to 60% during the same time period. After one year, the loss of breaking strength of the first set was the highest at Long Beach followed by Burbank and Upland which had very similar results. By far the lowest damage was observed at the background site (Salinas).

3.2 Definition of Exposure Groups

For the most part, all materials were exposed in groups and removed as groups. For purposes of the data analysis, an exposure group is defined as a set of coupons which were placed in the field at each site at about the same time and collected at about the same time. The exact timing of the start and end of the exposure group varied from site to site. Figure 3-17 gives the definitions of the exposure groups that were used in the data analysis. The starting dates in the Figure are approximate. For

the calculation of corrosion rates, the actual number of days of exposure for each material at each site was used.

Generally, all materials at a site were exposed and removed at the same time. An exception to this are the Al coupons, which were not exposed before the summer of 1987. Thus Al weight loss data are available along with the other materials only for groups 10, 11, 14, 15, 16, and 17. Furthermore, some Al coupons were deployed for periods that were different from those for the other materials. These periods are shown as exposure groups 18 and 19 in Figure 3-17.

The data analysis is based on the corrosion rate, i. e., the weight loss divided by the number of days the coupon was exposed. In order to obtain corrosion rates in g/m^2-year from weight loss rates in mg/day the exposed sample area (310 cm^2) has to be taken into account. Furthermore, the the rate of thickness loss in μm/year is obtained by dividing the numerical value of the corrosion rate given in g/m^2-year by the density of the material. Thus, the conversion factor from mg/day to μm/year turns out to be 11.77/density. Before presenting the statistical analysis of the corrosion rates, it is appropriate to consider whether or not the corrosion rate is an appropriate measure of damage.

3.2.1 Validity of Corrosion Rate as a Measure of Damage

Weight loss itself is not a convenient measure of damage for use in a statistical analysis. Obviously, the longer the exposure period the larger the weight loss. Thus, any statistical analysis must include exposure length as an independent variable in the regression. In this case, physical considerations lead to a dependence on time raised to a power. The exponent of time should be either one or one half, as explained in Section 3.1, Equation 2a.

One way to test the validity of the linear dependence of weight loss on time for Ni and Zn is to compare weight loss for the difference of two exposure groups with an exposure group which covers the same period. For example, in Figure 3-17 it is easy to see that the difference of groups 1 and 2 should give the same weight loss as group 5, if the corrosion rate is indeed constant. Figure 3-18 shows all such comparisons for Ni and Zn. Although the Zn weight loss shows considerable scatter, both materials show a strong linear trend which confirms that the corrosion rates for Zn and Ni are consistent among the exposure groups and that weight loss rate is a good measure of corrosion in this data set.

The following analysis of corrosion rate data assumes that the exponent of time is unity for all materials (b = 1). As shown

above, this is certainly true for Ni and Zn, but it is not the case for the paint samples. A time dependence with power 0.5 is closer to the truth for these materials. Thus, the paint weight loss was normalized in two ways, simply by time and by the square root of time. In either case, regression of the normalized weight loss on air quality and meteorology variables found no significant relationships.

3.2.2 Site-by-Site Comparison

Table 3-3 gives the results of a one-way analysis of variance of the corrosion rates for each material by site. The Table gives the mean value and 95% confidence interval for each site. The size of the 95% confidence interval is based on the pooled estimate of the error determined from the one-way analysis of variance. Basically, if 95% confidence intervals do not overlap then it is likely that the two sites are significantly different for that material. Note that this is not a formal statistical test, but a good indicator of significant differences nonetheless. The most interesting general observation to be made about the site-by-site differences is that each material follows a different pattern; there is no typical pattern. The only obvious significant differences between sites were observed for Ni. These differences are what might be expected; the "background" site at Salinas has a significantly lower corrosion rate than the sites in Southern California. Among these sites,

corrosion rates at Burbank and Long Beach are about equal in corrosivity and greater than Upland.

For Zn (galvanized steel), Long Beach and Salinas have greater weight loss rates than Upland, with Burbank in between, although the only difference that may be statistically significant is between Upland and Long Beach. The high level of loss for Zn at Salinas is at variance with its status as a background site. Apparently, damage to Zn is not related to levels of primary pollutants such as SO_2 and NO_2 in the atmosphere, which are much lower at Salinas. Indeed, the regression analysis will show that Zn corrosion rates are related to photochemically produced secondary pollutants such as O_3, which can serve as indicator for the photochemical processes that also produce HNO_3.

Finishing up the discussion of the metals, the Al corrosion rates may be significantly higher at Long Beach than Upland, but there are no other indications of any significant differences between the sites with respect to Al corrosion rate.

The two paint materials differ in the amount of added carbonate extender. Both are low carbonate paints, but one was lower in this reactive component than the other. Table 3-3 shows that there are no significant differences in weight loss rate between the sites for the L-C paint. As for the H-C paint, corrosion rates at Long Beach may be significantly greater than Salinas,

which would be consistent with the much higher SO_2 concentration at Long Beach and the fact that the H-C paint should be more susceptible to damage from acidic gases than the L-C paint.

Like the H-C paint, the damage rate for nylon is greatest at Long Beach and lowest at Upland. A reasonable physical explanation of this difference is not obvious since nylon is attacked by nitric acid, which is lower at Long Beach than at Upland. It is possible that the difference is not real but a statistical artifact of the small sample size.

3.3 Air Quality and Meteorological Variables

3.3.1 Data Sources

Air quality data related to this project were obtained from the California Air Resources Board (CARB) as monthly mean hourly concentrations for carbon monoxide (CO) in units of parts per million, and sulfur dioxide (SO_2), nitrogen dioxide (NO_2), oxides of nitrogen (NO_x), and ozone (O_3) in units of parts per hundred million for each of the four sites.

The relative humidity (RH) and related data were derived from standard meteorological data reports of hourly observations from airports near the four exposure sites. The data were obtained on

magnetic tape from the National Aerometric Data Bank for the airports at Burbank, Long Beach, Salinas, and Ontario, which is near Upland. Observations of temperature and the dew point are reported every hour; these were converted at USC to relative humidity data. The data capture at all stations except Long Beach is very good, with only a few random periods of missing data. At Long Beach, however, observations from midnight to five o'clock in the morning are missing for most of the study period. This data gap was filled by linear interpolation. Since the relative humidity at Long Beach during the early morning is almost always quite high and fairly constant, linear interpolation probably does not affect the frequency of occurrence of relative humidity, which is what is used in the data analysis.

3.3.2 Site-by-Site Comparison

Figure 3-19 through Figure 3-22 give the monthly average concentrations of SO_2, NO_2, O_3, and RH at the four sites. This last Figure clearly demonstrates that the highest humidities occur at Salinas and that the sites in the Los Angeles basin show major differences among each other.

Table 3-4 gives the one-way analysis of variance for air quality and meteorological variables that were found to be significantly related to weight loss. Unlike the corrosion rates, there are

many significant differences between the sites.

The concentration of the acidic gases, SO_2 and NO_2, at the background site Salinas is significantly lower than at the Southern California sites. In general, the between-site differences of these gases are consistent with known primary emissions. Long Beach and Burbank have levels of SO_2 that are very low by most standards, but elevated relative to Upland and Salinas probably because of nearby, large electric generating stations. The very high levels of NO_2 at all Southern California sites is obviously caused by the enormous amount of motor vehicle exhaust as compared to Salinas (or anywhere else).

O_3, which is an indicator of photochemical smog intensity, is lowest at Long Beach because its coastal location puts it upwind of O_3 precursor emissions in the summer. The levels of O_3 at Salinas are about the same as at Burbank. Thus, Salinas is not as much of a background site for ozone as it is for SO_2 and NO_2. Perhaps Salinas also has significant levels of other photochemically created species such as HNO_3 and hydrochloric acid (HCl). Direct measurements of these species are not available at Salinas, however, therefore this is a conjecture.

The only meteorological variables that were found to be related to corrosion rate in this study were T60 and T60-T80. T60 is the fraction of the time that the relative humidity was greater than

60 percent. T80 is similarly defined, thus T60-T80 is the time the RH is between 60 and 80 percent. T60-T80 can be considered a measure of extended high humidity periods. The results here are predictable: T60 is high at Long Beach, which is very near the ocean and Salinas, which is further from the ocean than Long Beach, but is located near the ocean at the mouth of the Salinas river. Upland, the site furthest inland, has the lowest T60. Burbank, which is located in the San Fernando Valley, has T60 values that are midway between those for Long Beach and Upland. Like T60, analysis of T60-T80 values shows that these are determined by the degree of marine influence. Thus, the two coastal sites have the highest values.

To close this section, HNO_3 concentrations are discussed. During the first phase of this project HNO_3 was measured by absorption on a nylon filter. Monthly concentrations for the period March 1986 to March 1988 are reported in the final report of that project (5). However, comparison of these data with HNO_3 data taken by Cal Tech led to the conclusion that the data were unreliable probably because of problems with the sampling method. As a result, the HNO_3 measurements taken as a part of this project have not been used in later statistical analyses of the corrosion rates.

The best available long term measurements of HNO_3 are from the initial phase of the CARB's California Acid Deposition Monitoring

Program (CADMP) (5). Of the three sites in the Los Angeles basin for which concentrations are reported, only the Long Beach site is coincident with a materials damage exposure site. The CADMP site at Azusa is comparable to the Upland site. However, the CADMP site in downtown Los Angeles is probably not a good match for the Burbank exposure site. For the period from 6 October 1988 through 25 September 1989, the average HNO_3 concentrations at Long Beach, downtown Los Angeles, and Azusa were 1.57, 3.00, and 3.02 $\mu g/m^3$, respectively. These concentrations are much lower than the average concentrations measured during the first phase of this project, which is another reason to doubt the validity of the HNO_3 monitoring in the first phase. The CADMP data show HNO_3 levels to be much higher in the day than the night, consistent with the photochemical production of HNO_3 during the day and its rapid deposition at night. The seasonal variation of HNO_3 is similar to O_3, low in the winter and high in the summer.

3.4 Tables

Table 3-1 Precision of the Weight Loss Measurements Derived from Paired Samples

Species	Number of Pairs	Error Bars (2σ)
Zinc	63	± 24.6 mg
Nickel	63	± 14.8 mg
Low Carbonate Paint	63	± 23.2 mg
High Carbonate Paint	62	± 19.0 mg
Aluminum	43	± 7.2 mg

Table 3-2 Coefficients a and b in Equation 2 For All Materials and Sites

		Zn	Ni	Al	H-C	L-C
a	BR	81.5	77.3	29.2	123.7	68.1
	LB	107.9	76.9	43.6	135.8	66.4
	UP	60.9	48.4	17.1	106.3	57.1
	SL	82.8	25.1	38.6	86.4	51.4
b	BR	0.744	0.744	1.290	0.801	0.640
	LB	0.866	0.932	1.190	0.631	0.738
	UP	0.949	0.947	1.012	0.782	0.801
	SL	0.580	0.917	0.899	0.565	0.503

a is the weight loss (in mg) after one year;
b is a dimensionless parameter.

Table 3-3 Corrosion Rates by Site and Material

Zinc

SITE	N	MEAN
BR	16	0.2168
LB	16	0.2816
SL	15	0.2603
UP	16	0.1511

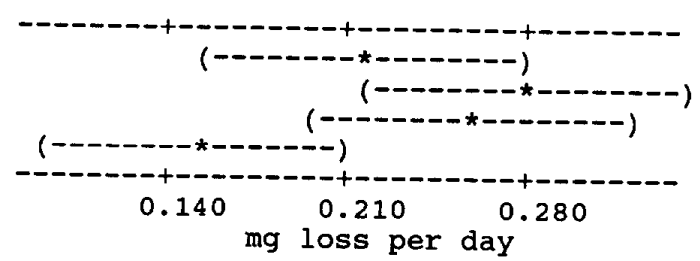

Nickel

SITE	N	MEAN
BR	16	0.22544
LB	16	0.22064
SL	15	0.07061
UP	16	0.13133

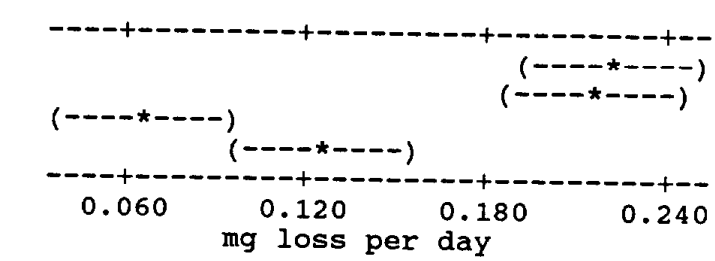

Low Carbonate Paint

SITE	N	MEAN
BR	16	0.2333
LB	16	0.2167
SL	15	0.1979
UP	16	0.1791

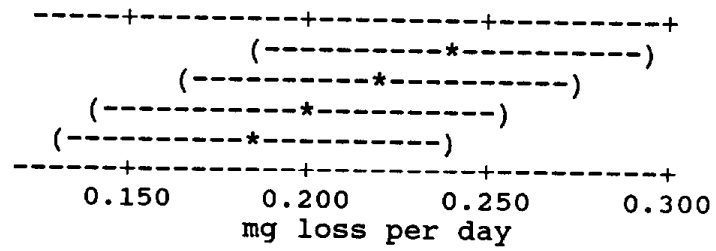

High Carbonate Paint

SITE	N	MEAN
BR	16	0.3723
LB	16	0.4063
SL	14	0.2824
UP	16	0.3346

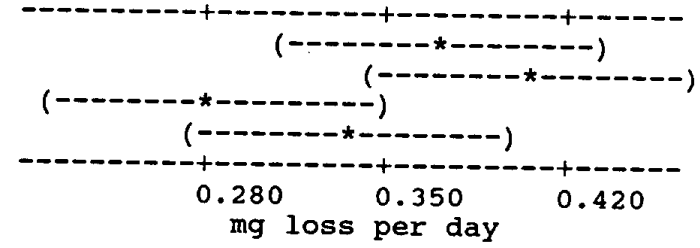

Aluminum

SITE	N	MEAN
BR	11	0.07633
LB	11	0.12644
SL	10	0.09001
UP	11	0.04628

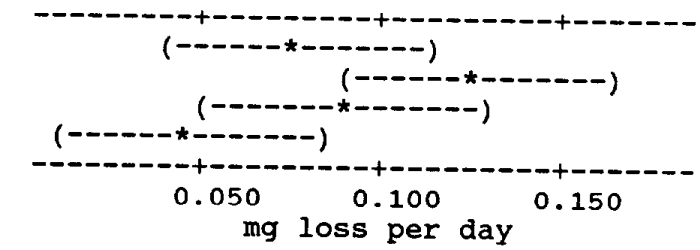

Table 3-3 (Cont.) CORROSION RATE BY SITE AND MATERIAL

Nylon Fabric

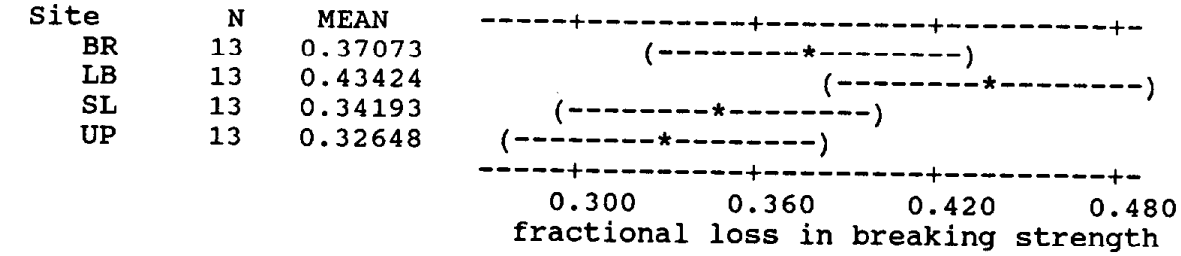

Ranges shown as (--*--) represent approximate 95% confidence intervals about the mean value based on the pooled standard deviation. Non-overlapping intervals may indicate sites with means that are significantly different (a t-test would be needed to confirm this). The coupon size is 310 cm^2, and the conversion factor from mg/day to μm/year is 11.77/(density of the material). Thus, the conversion factors for Al, Ni, and Zn are 4.359, 1.322, and 1.651, respectively.

Table 3-4 Important Air Quality and Meteorological Variables

SO_2

SITE	N	MEAN
BR	17	0.36159
LB	17	0.66535
SL	16	0.00767
UP	16	0.09802

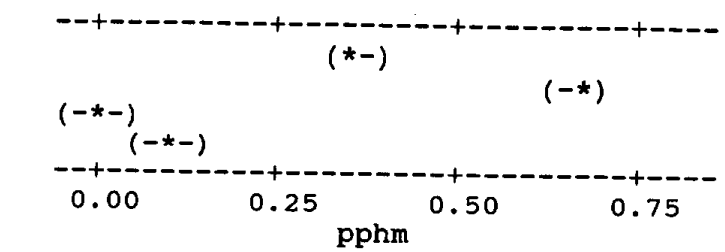

NO_2

SITE	N	MEAN
BR	17	5.3371
LB	17	4.6862
SL	16	1.3635
UP	16	4.4994

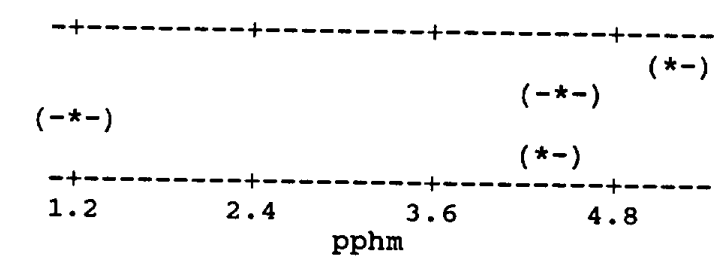

O_3

SITE	N	MEAN
BR	17	2.5210
LB	17	1.7667
SL	16	2.3013
UP	16	3.2233

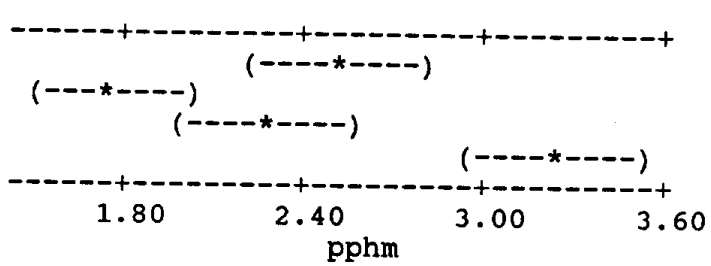

T60[a]

SITE	N	MEAN
BR	17	0.47651
LB	17	0.70713
SL	16	0.77855
UP	16	0.55946

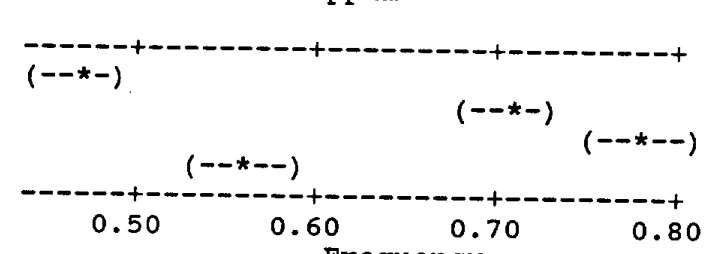

T60-T80[a]

SITE	N	MEAN
BR	17	0.30875
LB	17	0.35121
SL	16	0.35090
UP	16	0.26234

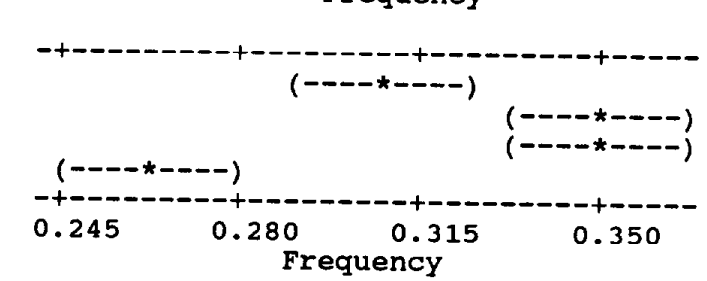

See Table 3-3 for explanation of ranges shown as (--*--).
a. T60 is the fraction of the period relative humidity is greater than or equal to 60%. T60-T80 is the fraction of the time humidity was between 60% and 80%.

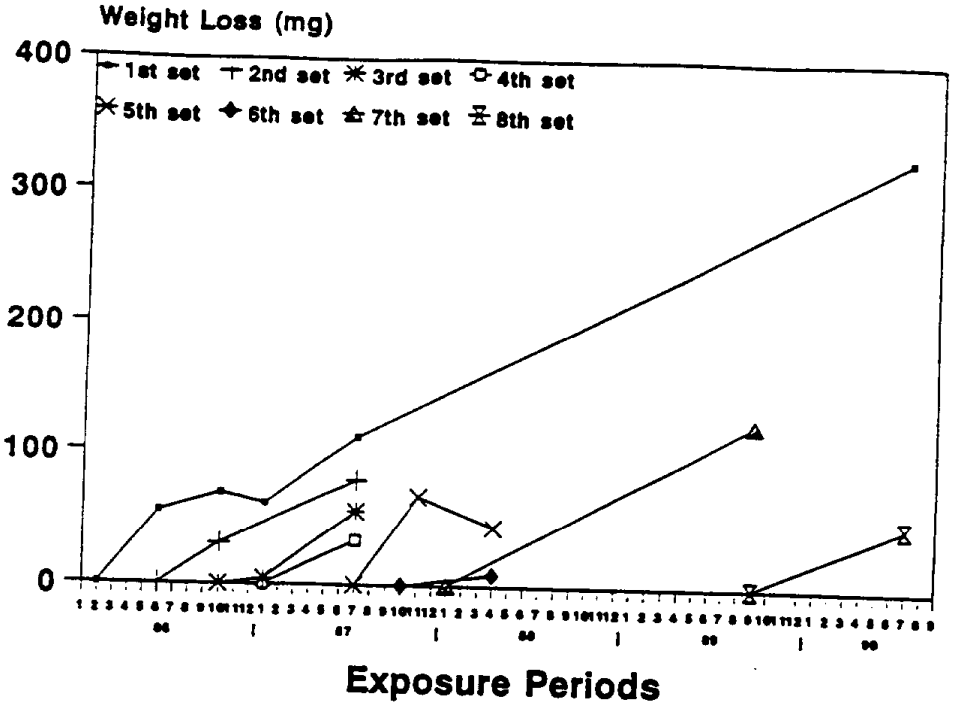

Figure 3-1 Weight loss for eight sets of galvanized steel as a function of exposure time at Burbank.

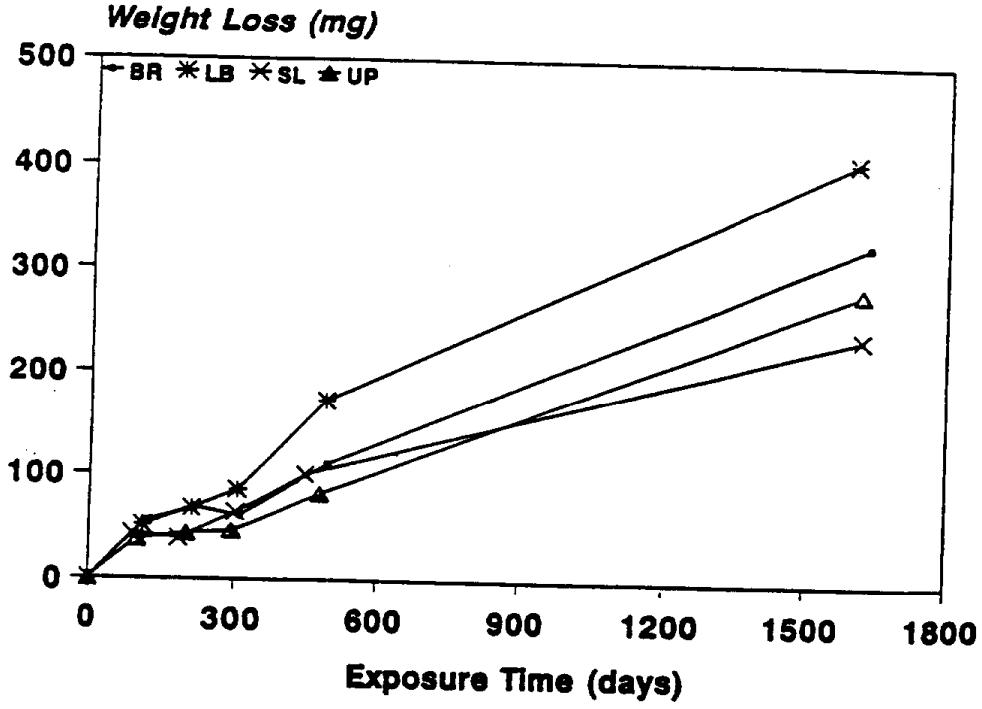

Figure 3-2 weight loss for the first set of galvanized steel as a function of exposure time at the four test sites.

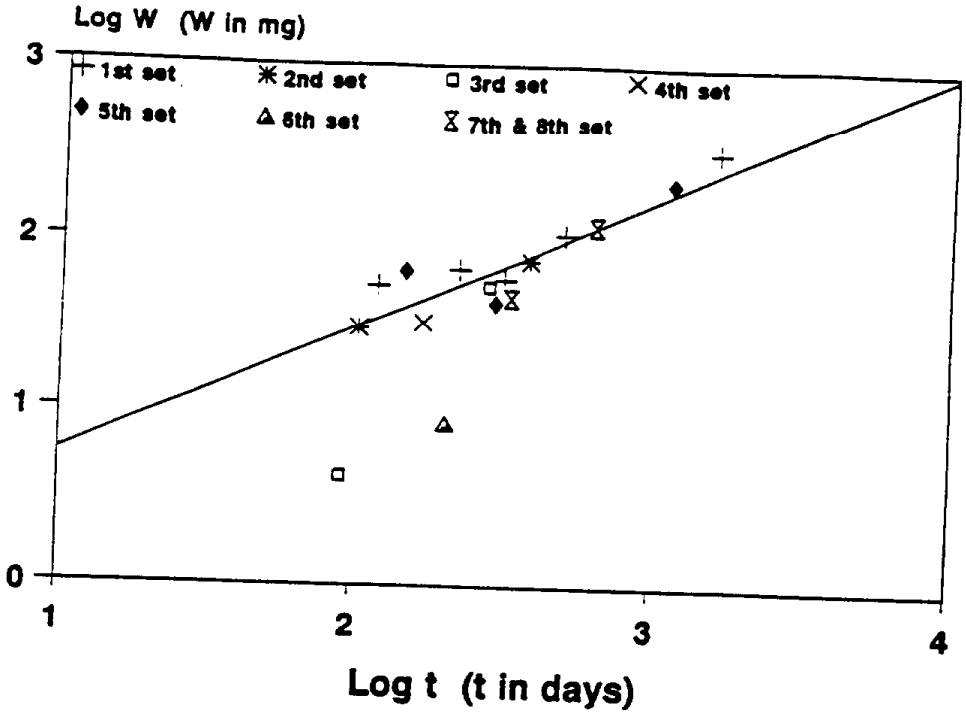

Figure 3-3a Plot of log W vs log t for galvanized steel at Burbank.

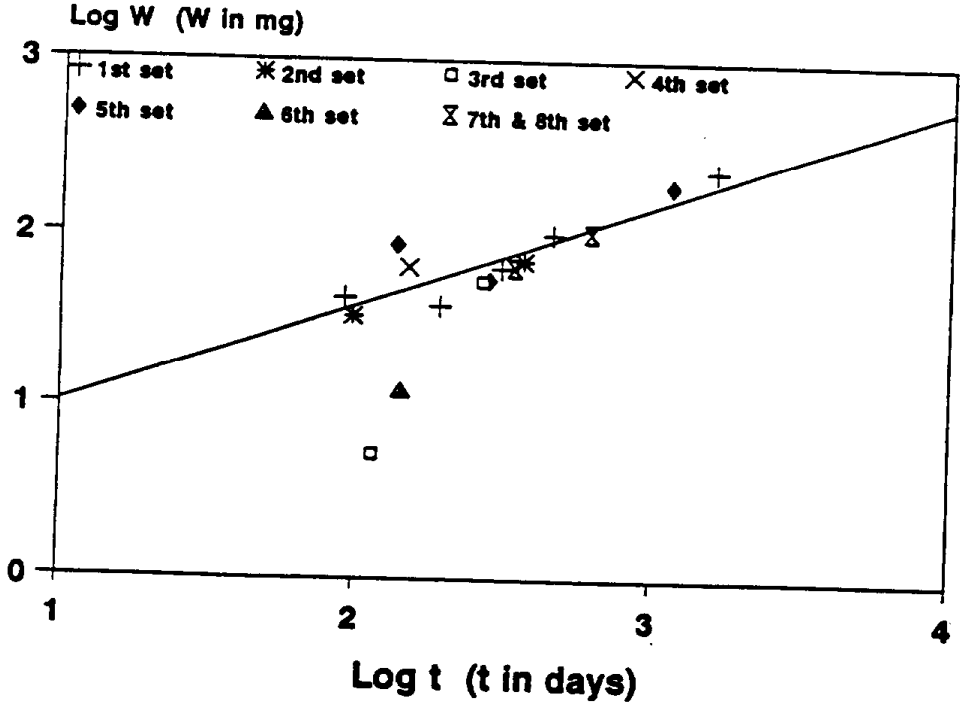

Figure 3-3b Plot of log W vs log t for galvanized steel at Salinas.

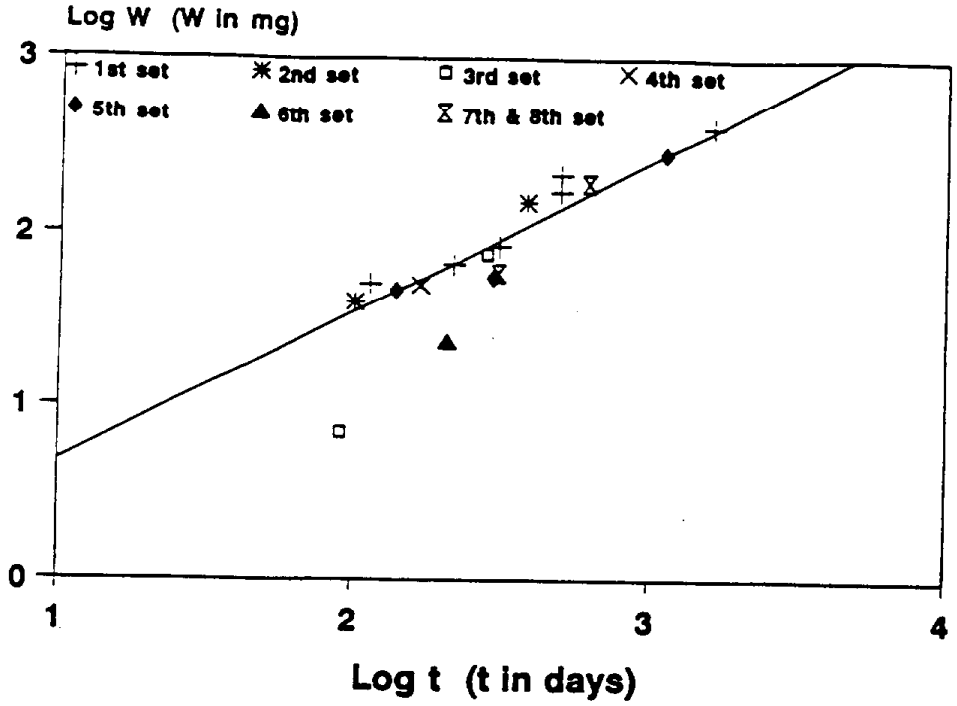

Figure 3-3c Plot of log W vs log t for galvanized steel at Long Beach.

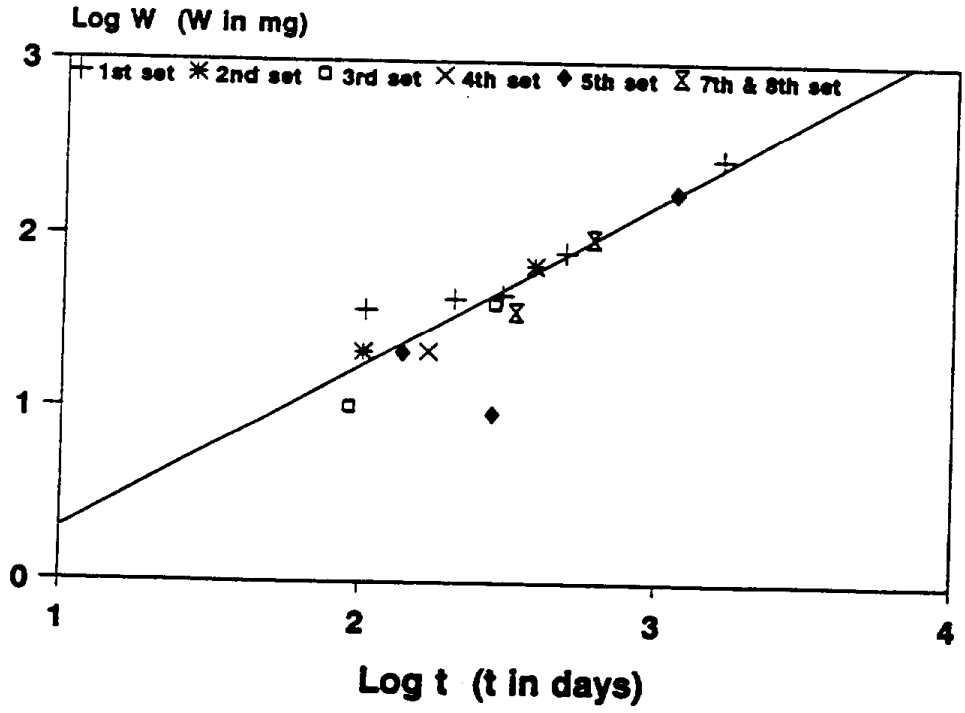

Figure 3-3d Plot of log W vs log t for galvanized steel at Upland.

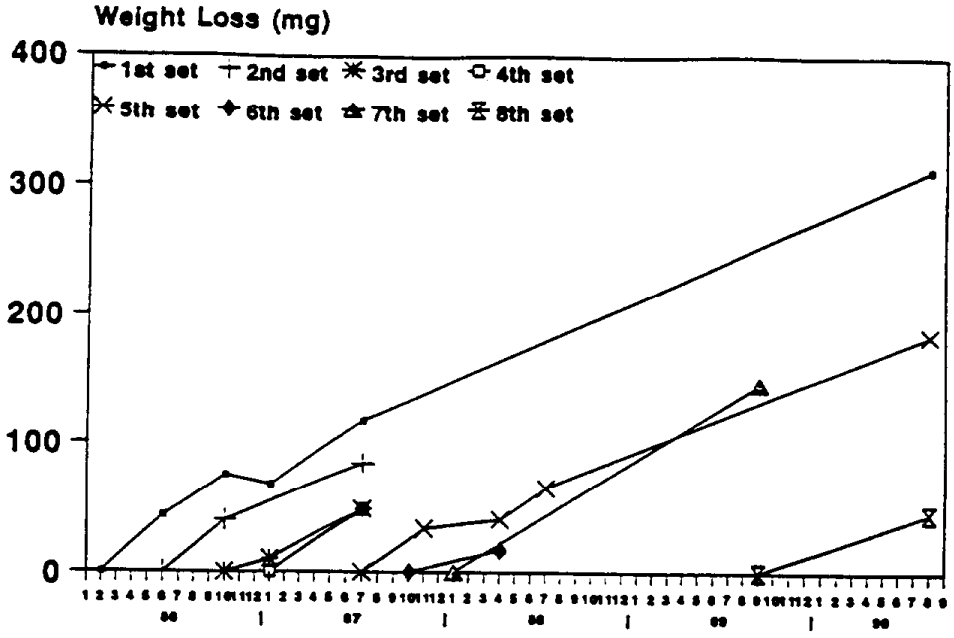

Figure 3-4 Weight loss for eight sets of nickel as a function of exposure time at Burbank

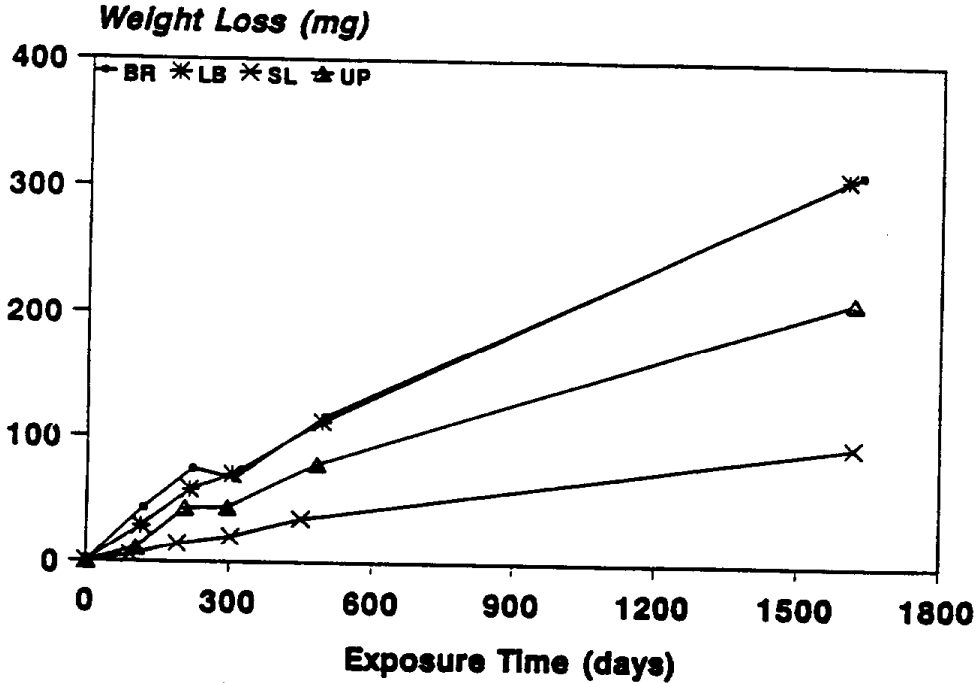

Figure 3-5 Weight loss for the first set of nickel as a function of exposure time at the four test sites

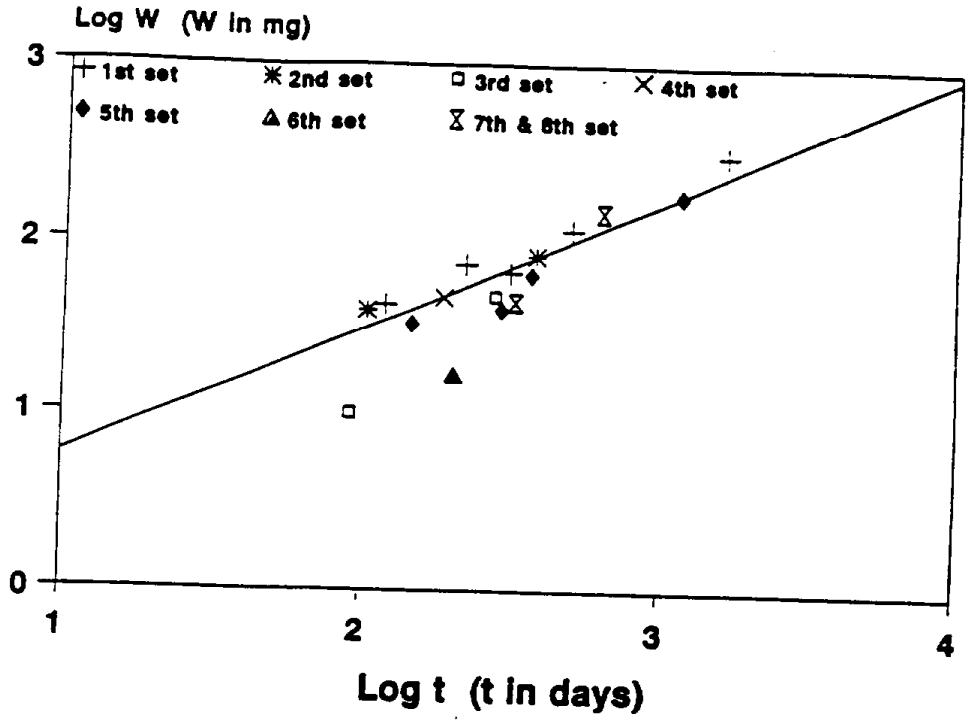

Figure 3-6a Plot of log W vs log t for nickel at Burbank.

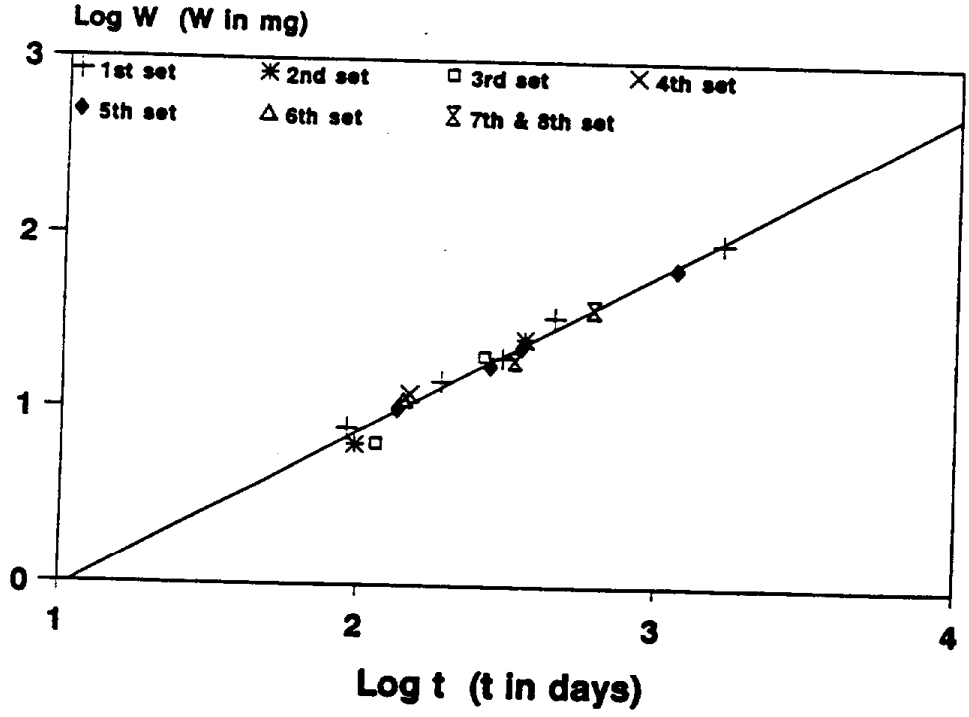

Figure 3-6b Plot of log W vs log t for nickel at Salinas.

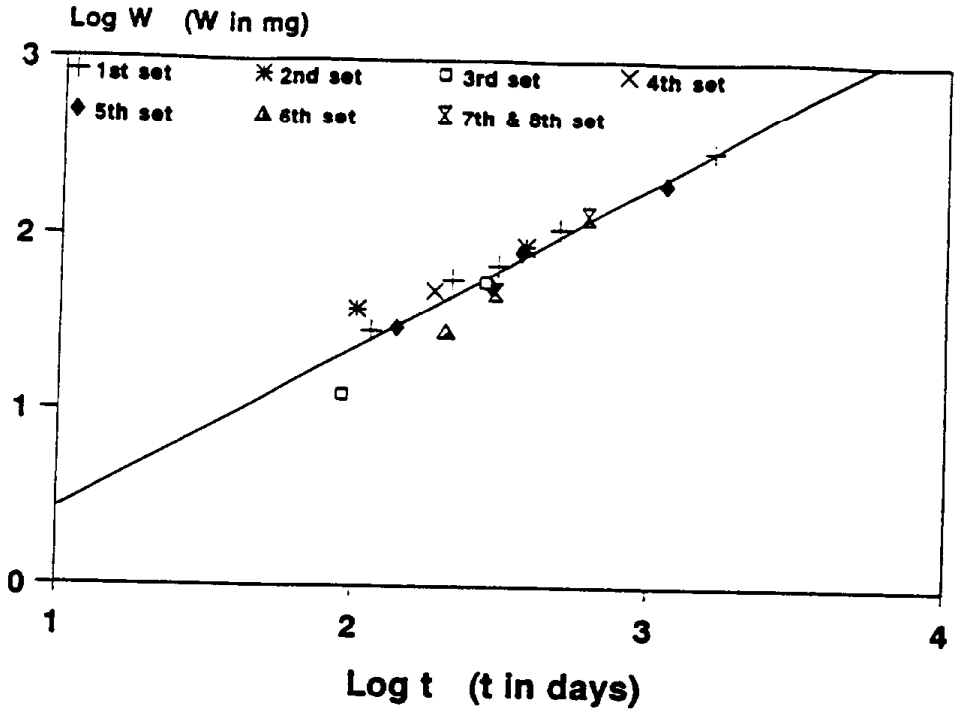

Figure 3-6c Plot of log W vs log t for nickel at Long Beach.

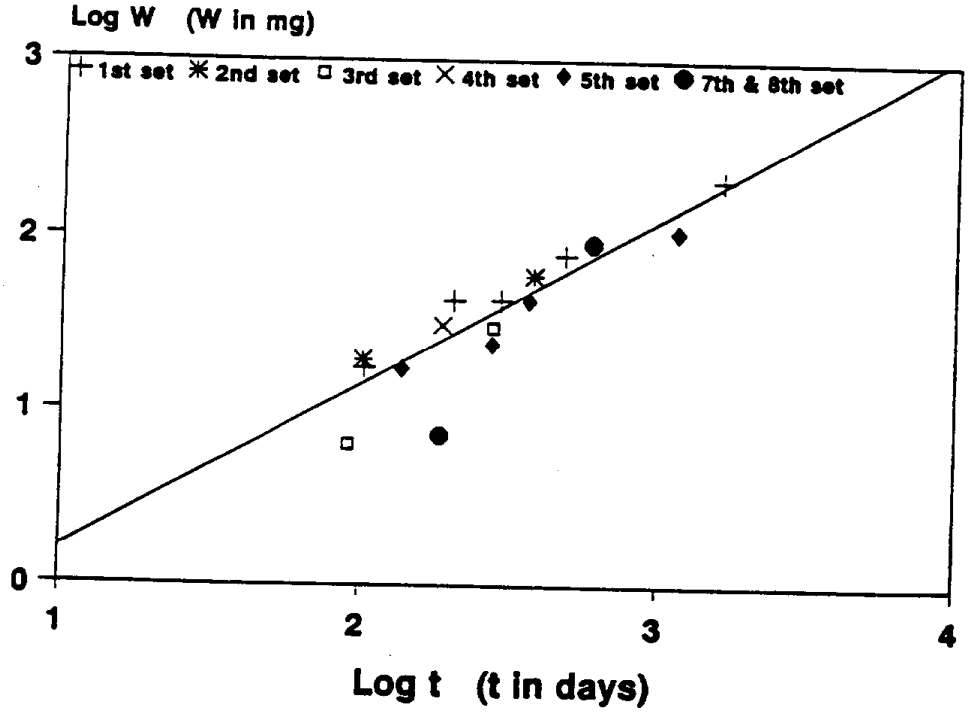

Figure 3-6d Plot of log W vs log t for nickel at Upland.

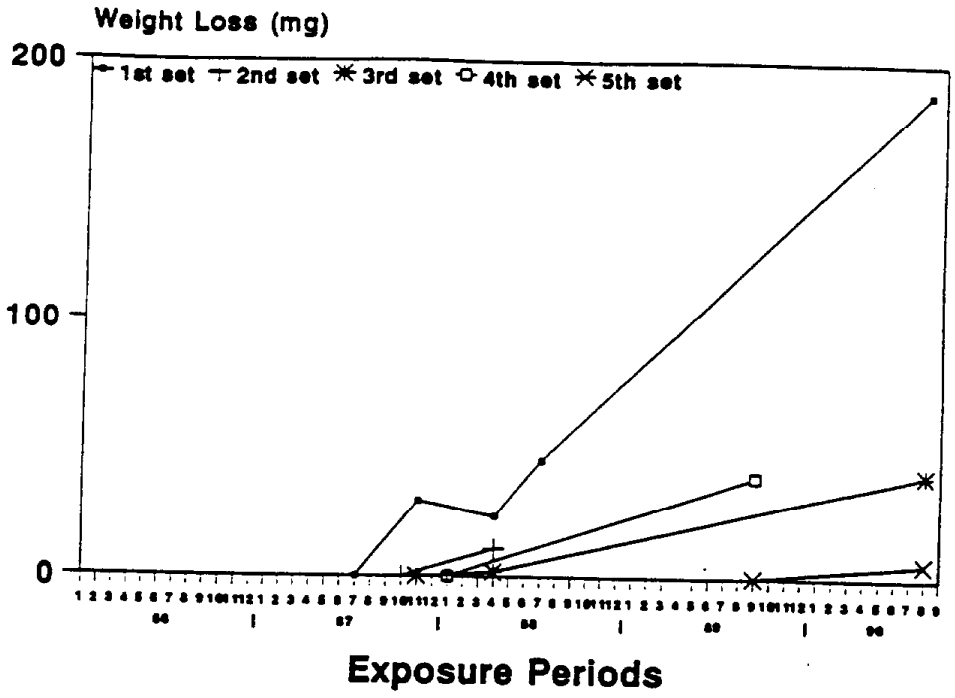

Figure 3-7 Weight loss for five sets of aluminum as a function of exposure time at Burbank.

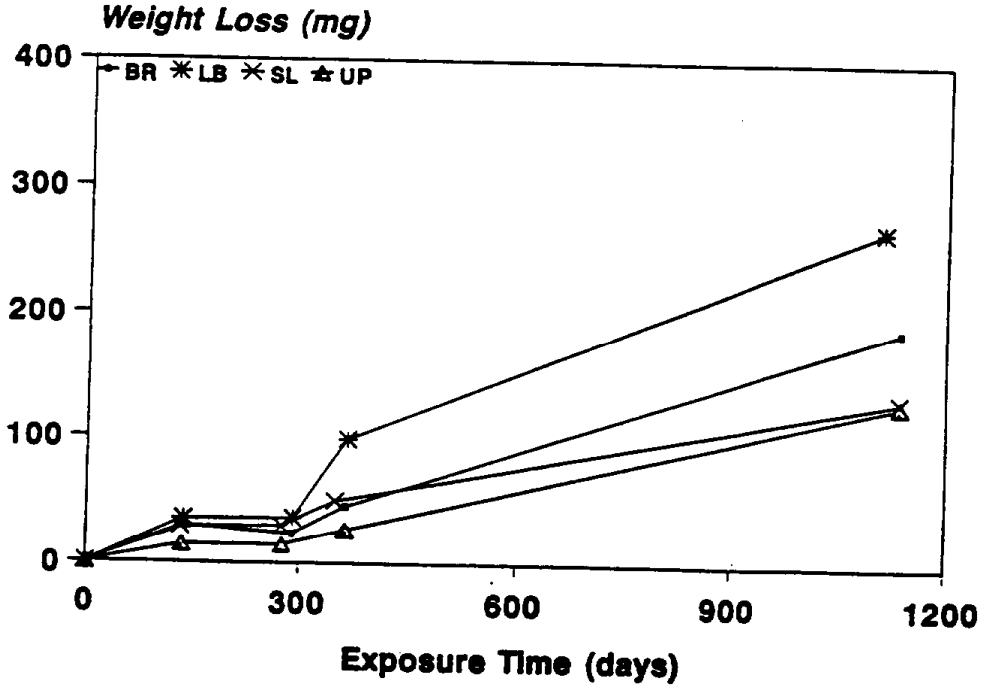

Figure 3-8 Weight loss for the first set of aluminum as a function of exposure time at the four test sites.

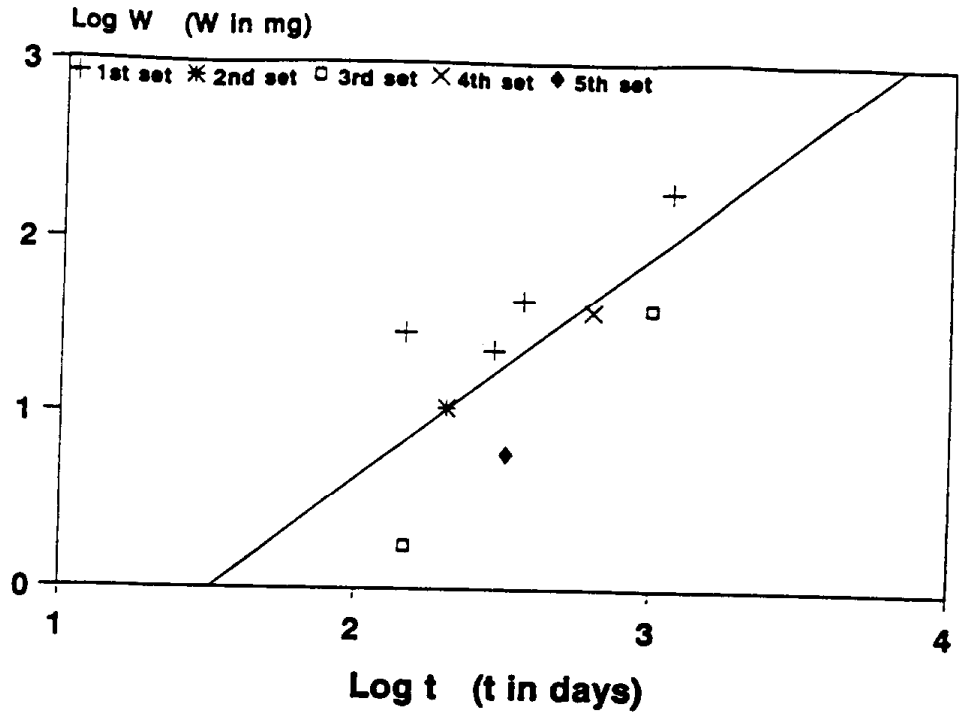

Figure 3-9a Plot of log W vs log t for aluminum at Burbank.

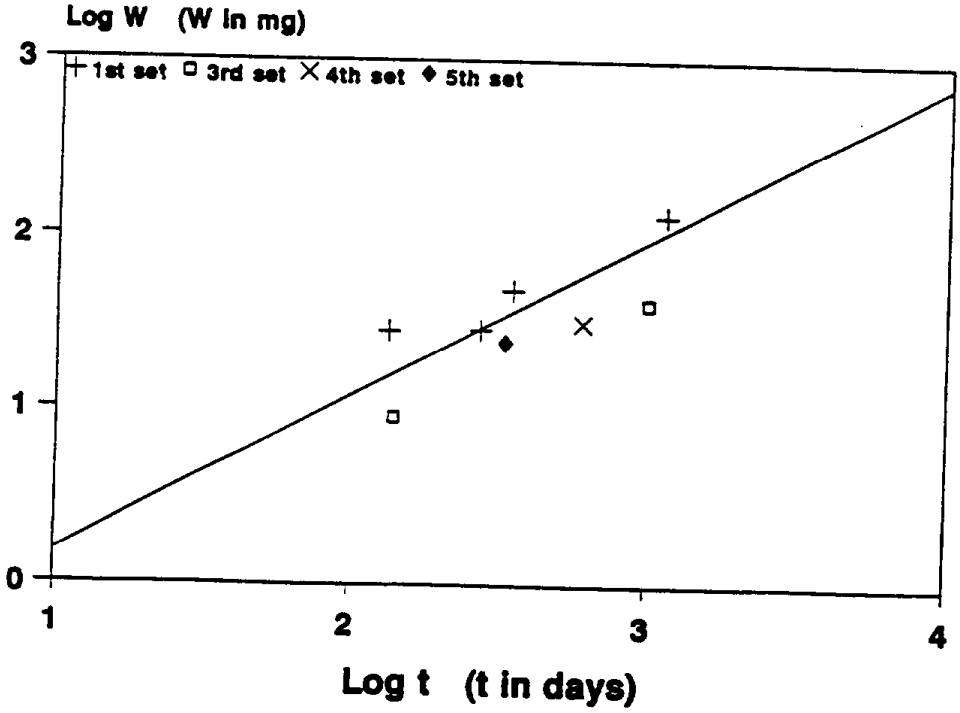

Figure 3-9b Plot of log W vs log t for aluminum at Salinas.

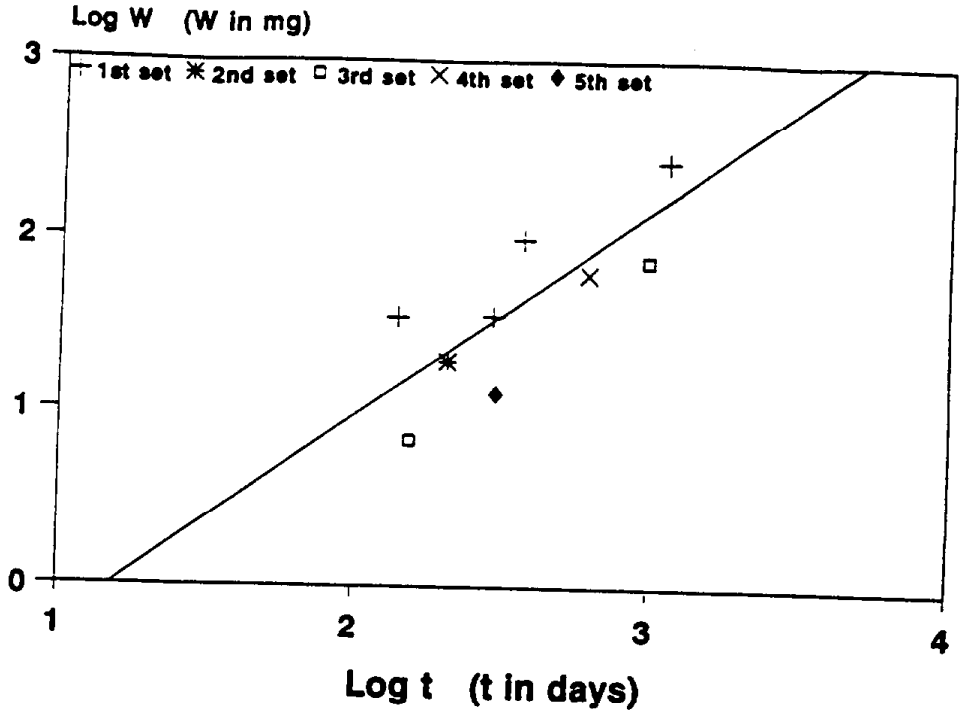

Figure 3-9c Plot of log W vs log t for aluminum at Long Beach.

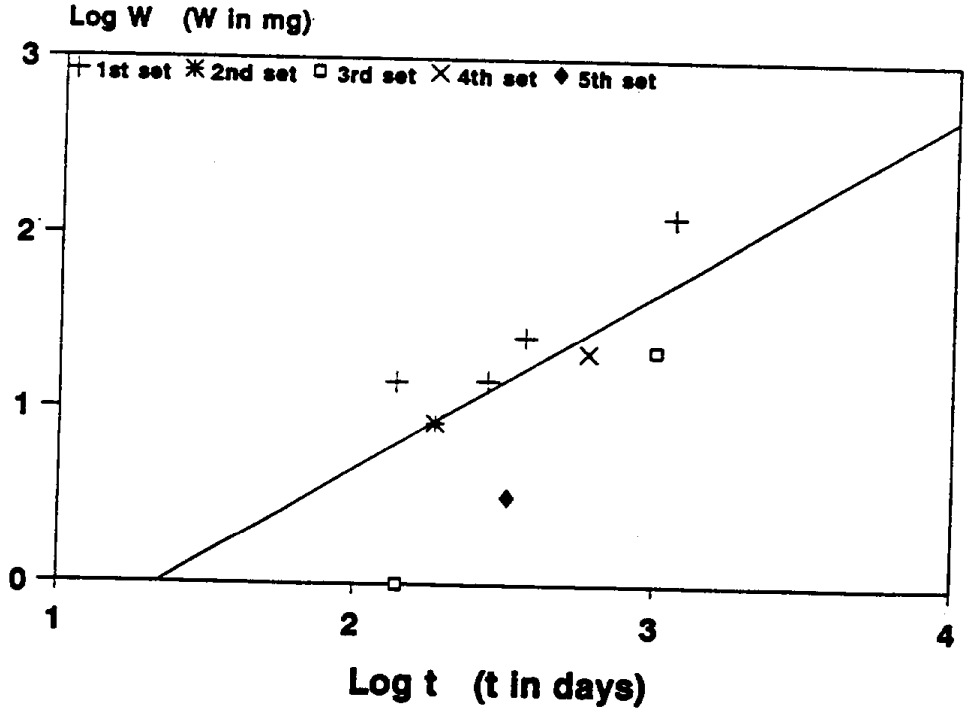

Figure 3-9d Plot of log W vs log t for aluminum at Upland.

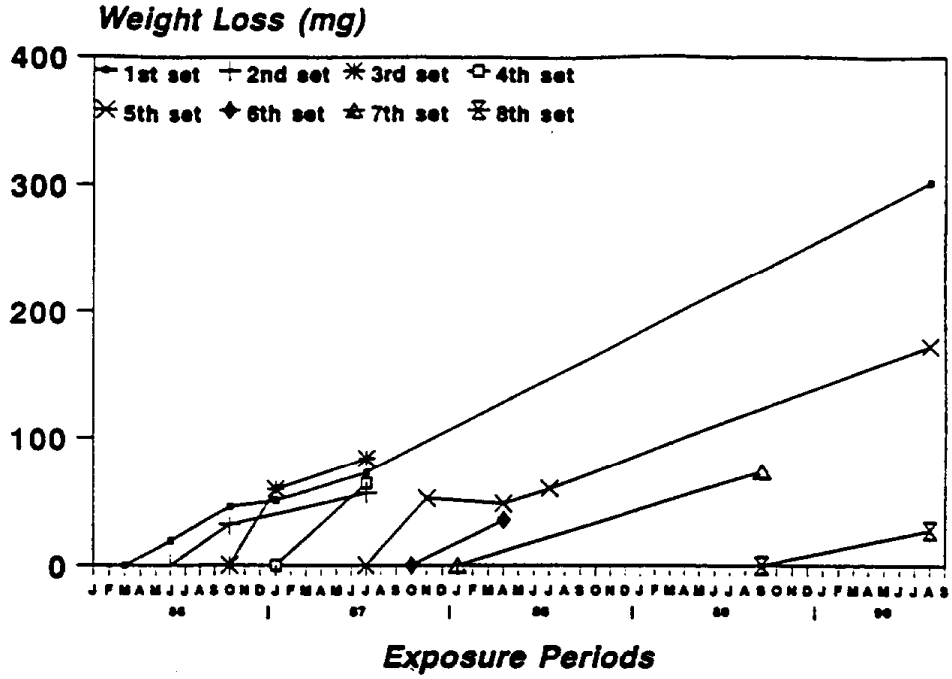

Figure 3-10 Weight loss for eight sets of L-C paint as a function of exposure time at Burbank

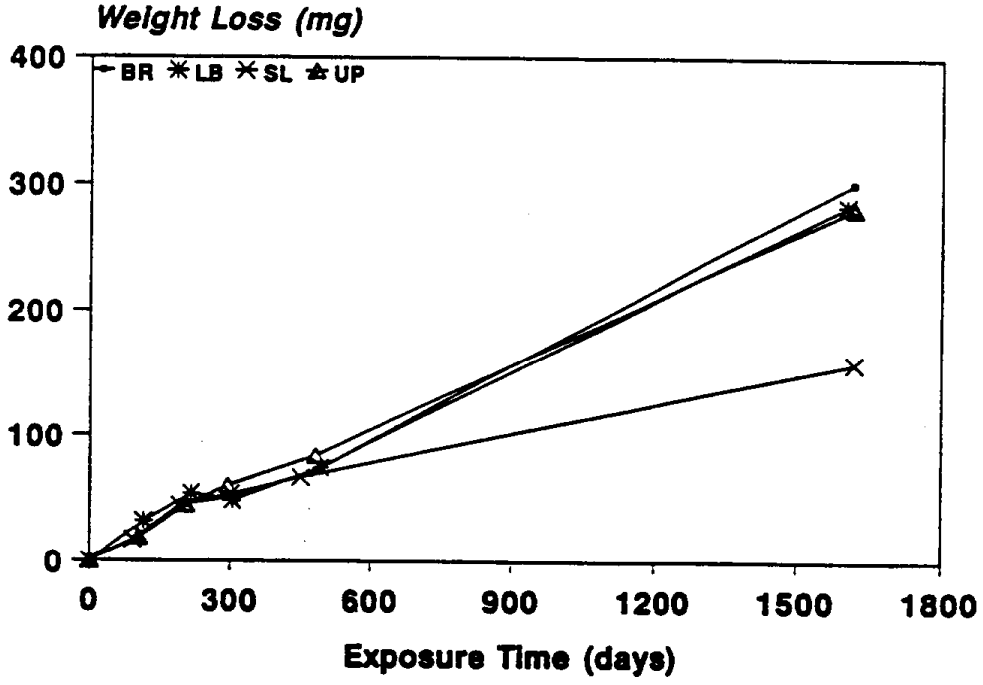

Figure 3-11 Weight loss for the first set of L-C paint as a function of exposure time at the four test sites

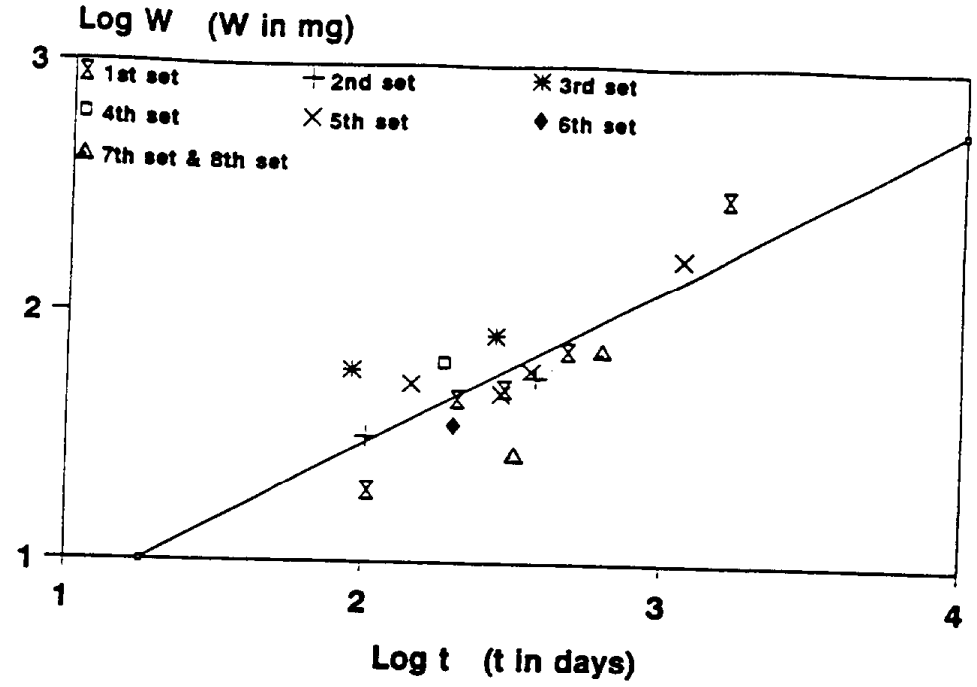

Figure 3-12a Plot of log W vs log t for L-C paint at Burbank.

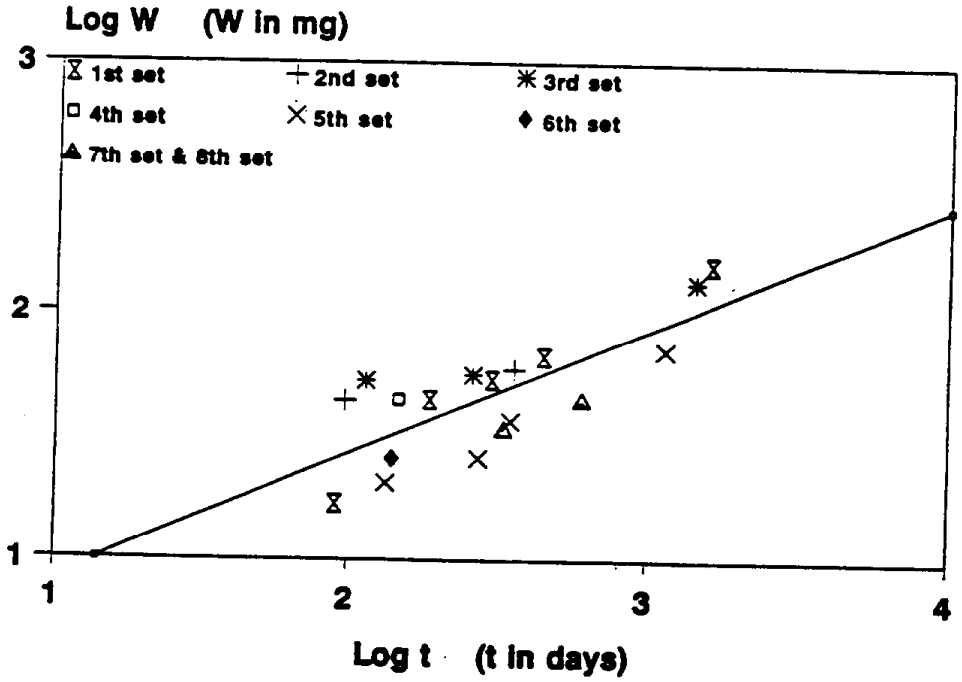

Figure 3-12b Plot of log W vs log t for L-C paint at Salinas.

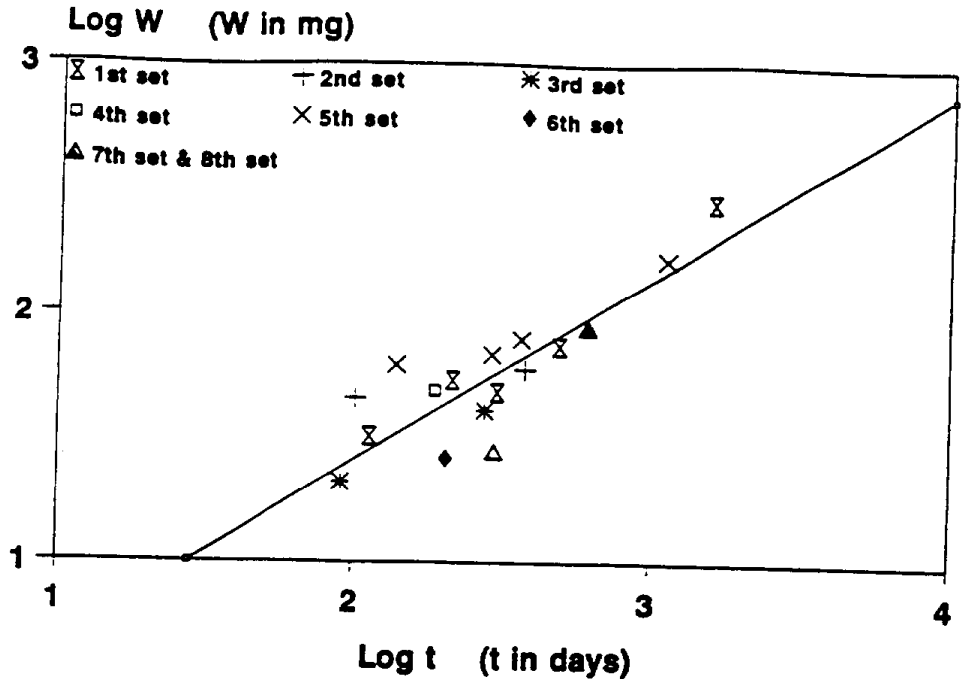

Figure 3-12c Plot of log W vs log t for L-C paint at Long Beach.

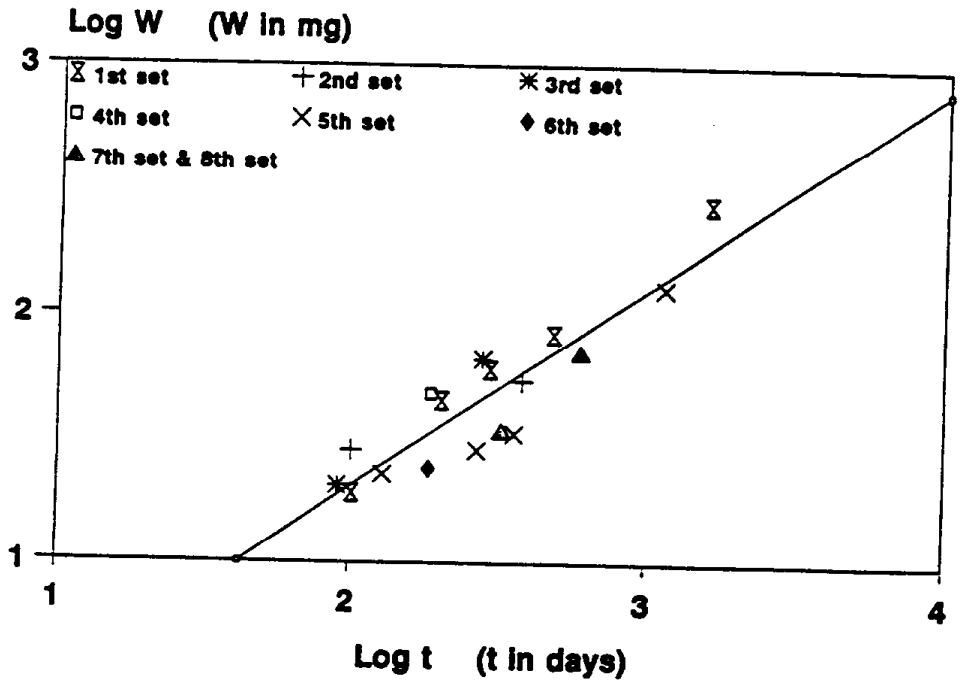

Figure 3-12d Plot of log W vs log t for L-C paint at Upland.

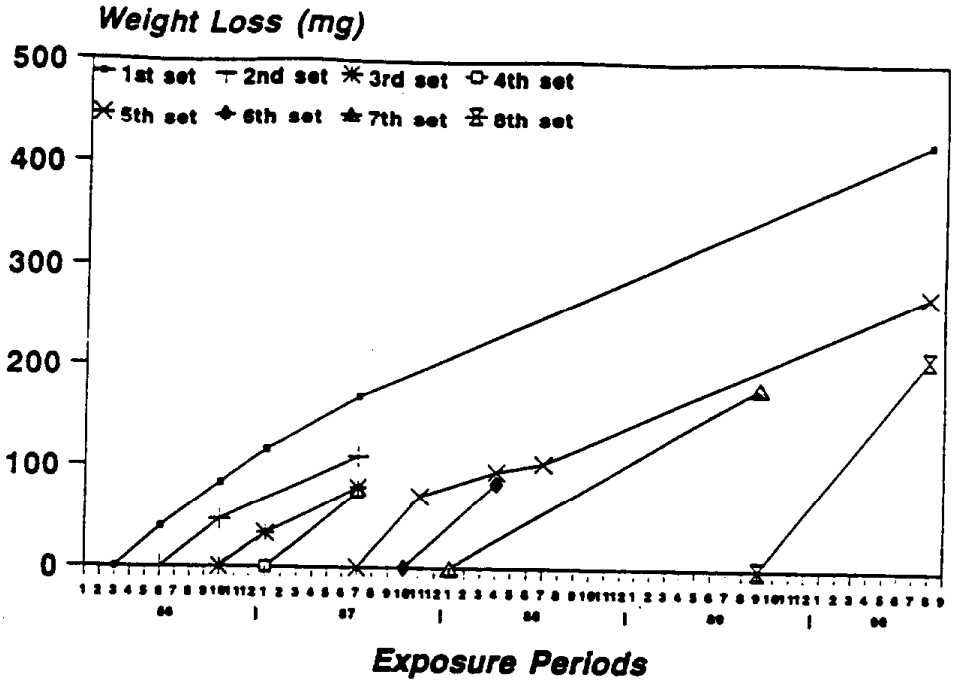

Figure 3-13 Weight loss for eight sets of H-C paint as a function of exposure time at Burbank

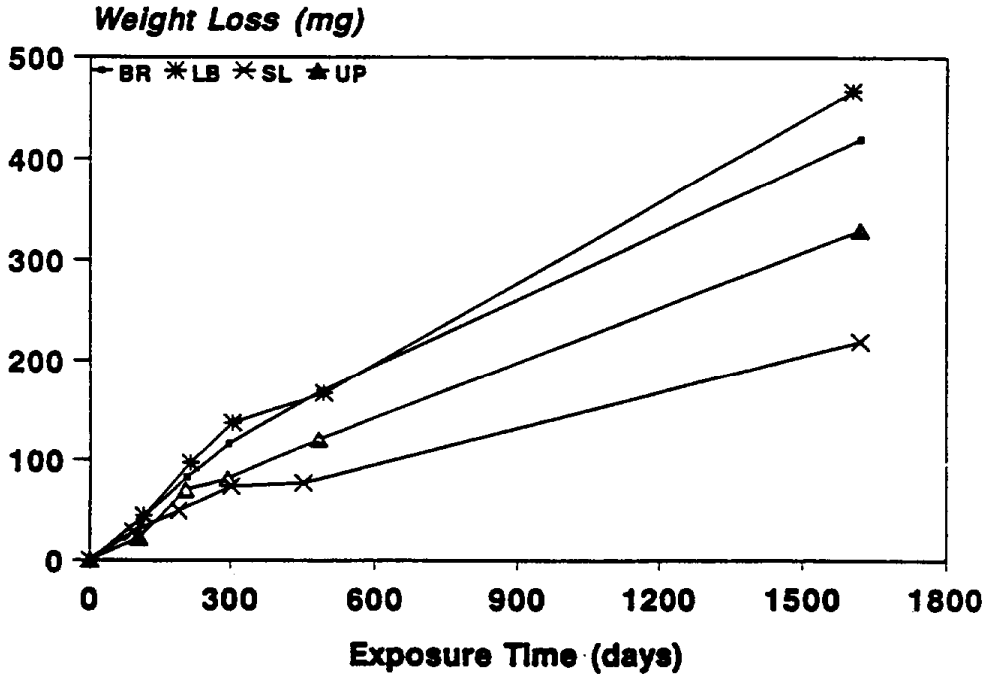

Figure 3-14 Weight loss for the first set of H-C paint as a function of exposure time at the four test sites

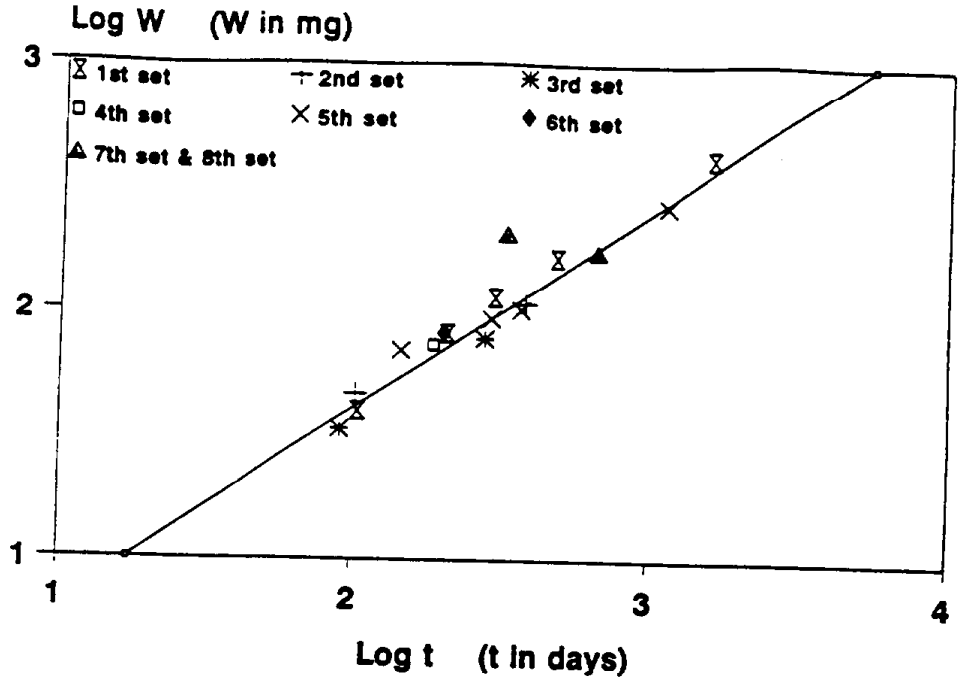

Figure 3-15a Plot of log W vs log t for H-C paint at Burbank.

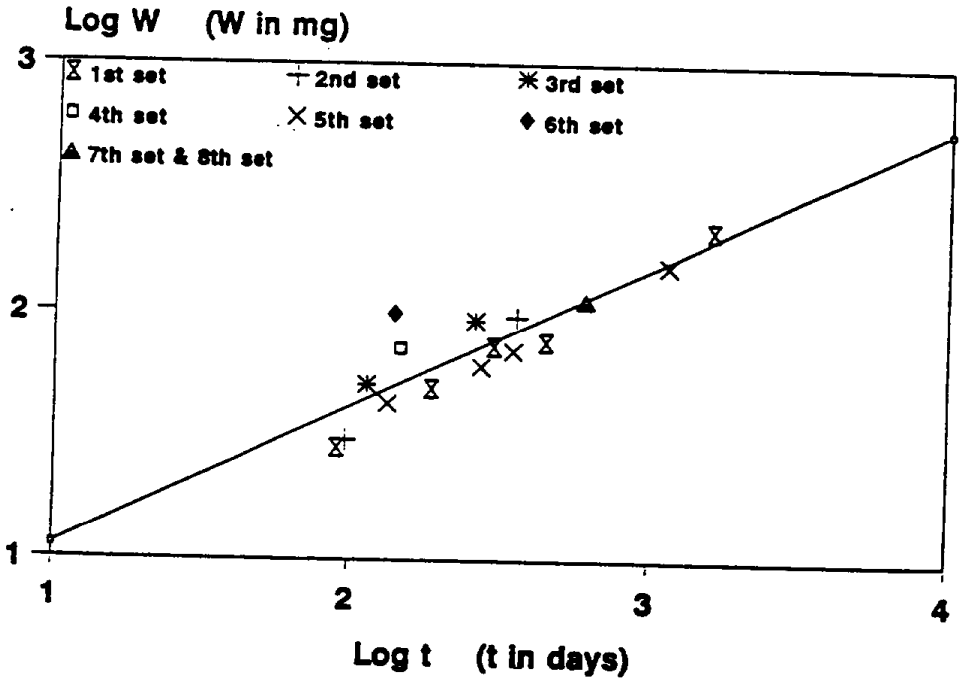

Figure 3-15b Plot of log W vs log t for H-C paint at Salinas.

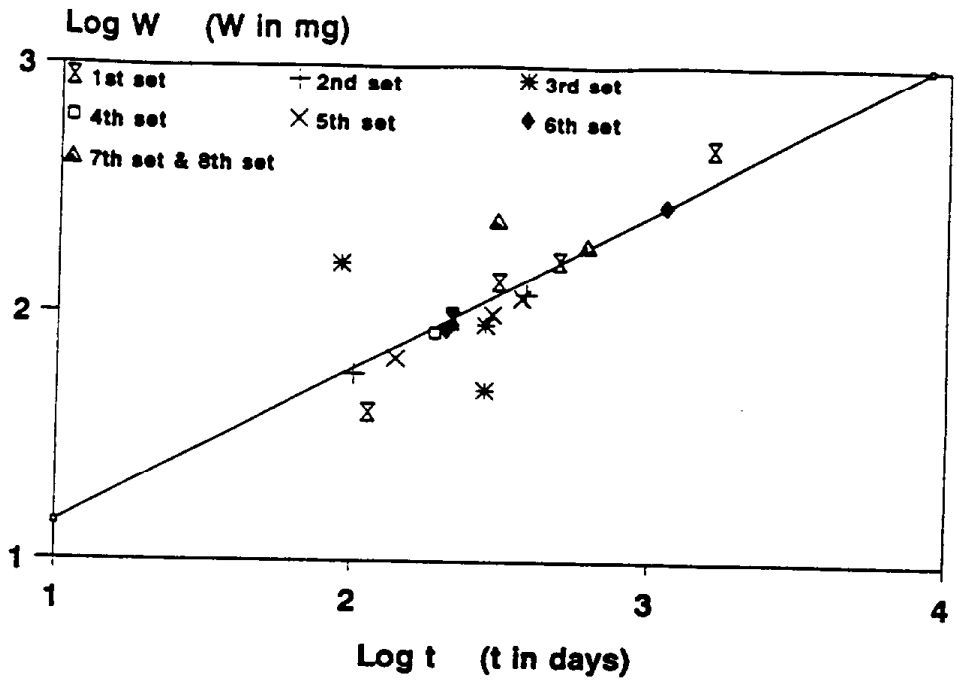

Figure 3-15c Plot of log W vs log t for H-C paint at Long Beach.

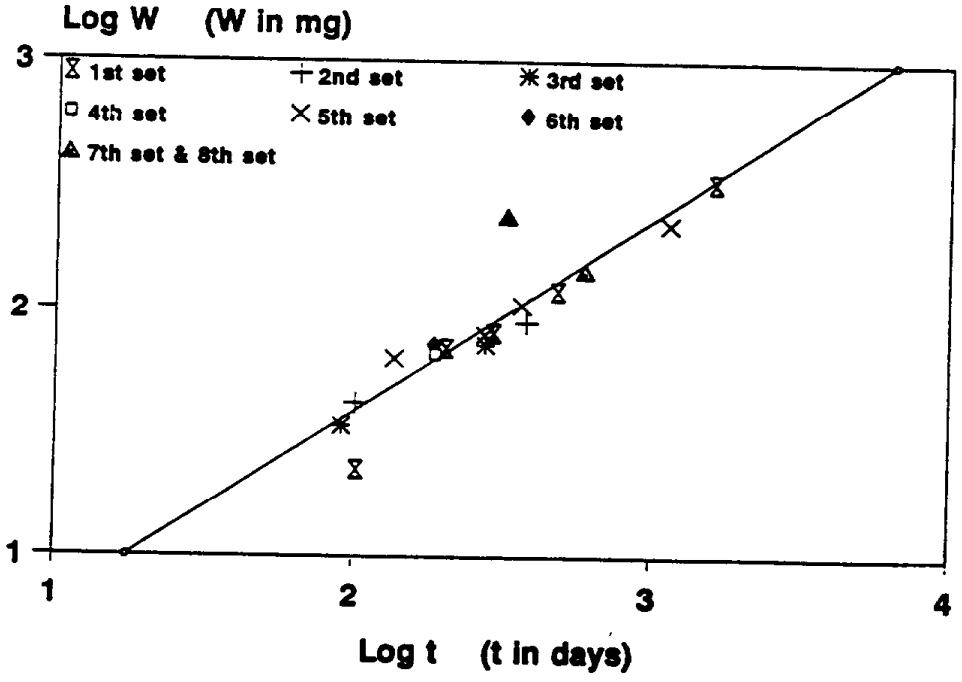

Figure 3-15d Plot of log W vs log t for H-C paint at Upland.

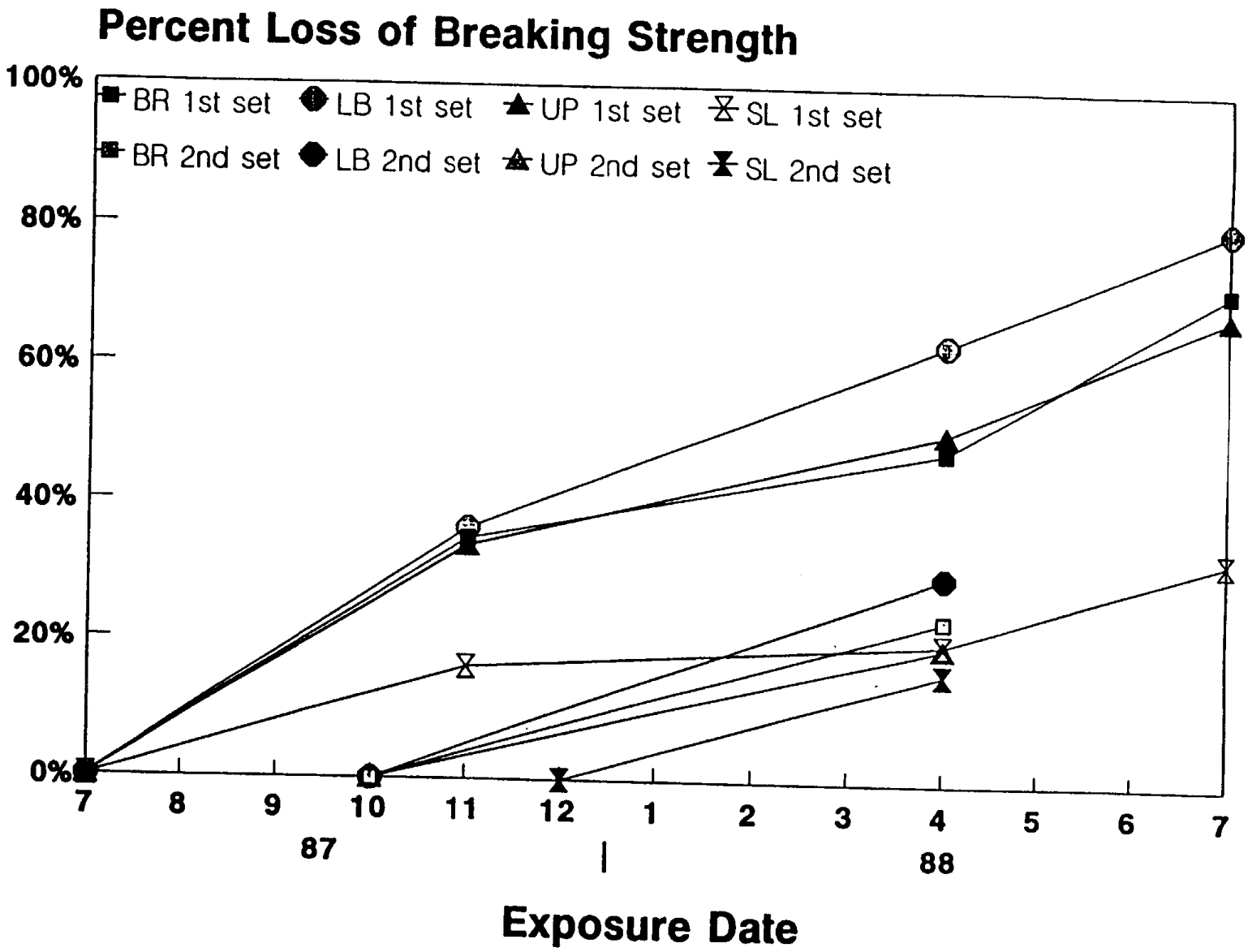

Figure 3-16 Loss of strength as a function of exposure time for two sets of nylon fabric at the four test sites

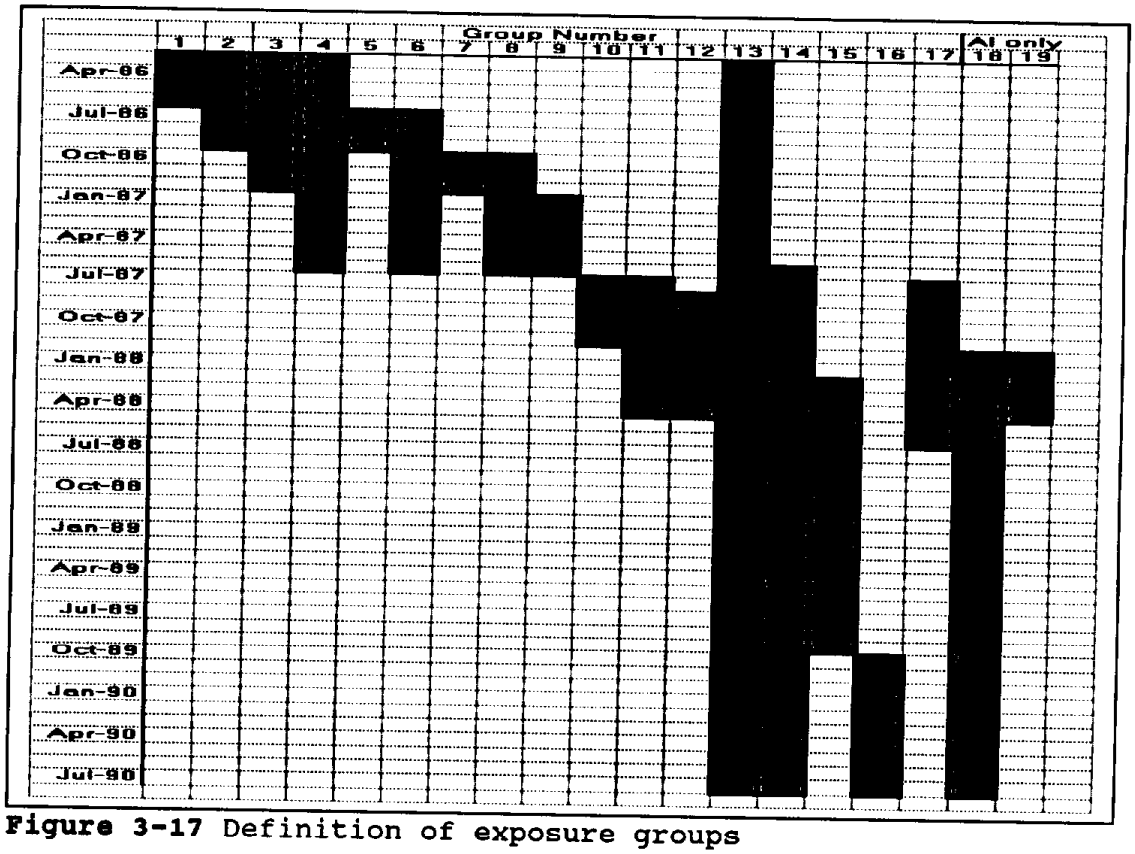

Figure 3-17 Definition of exposure groups

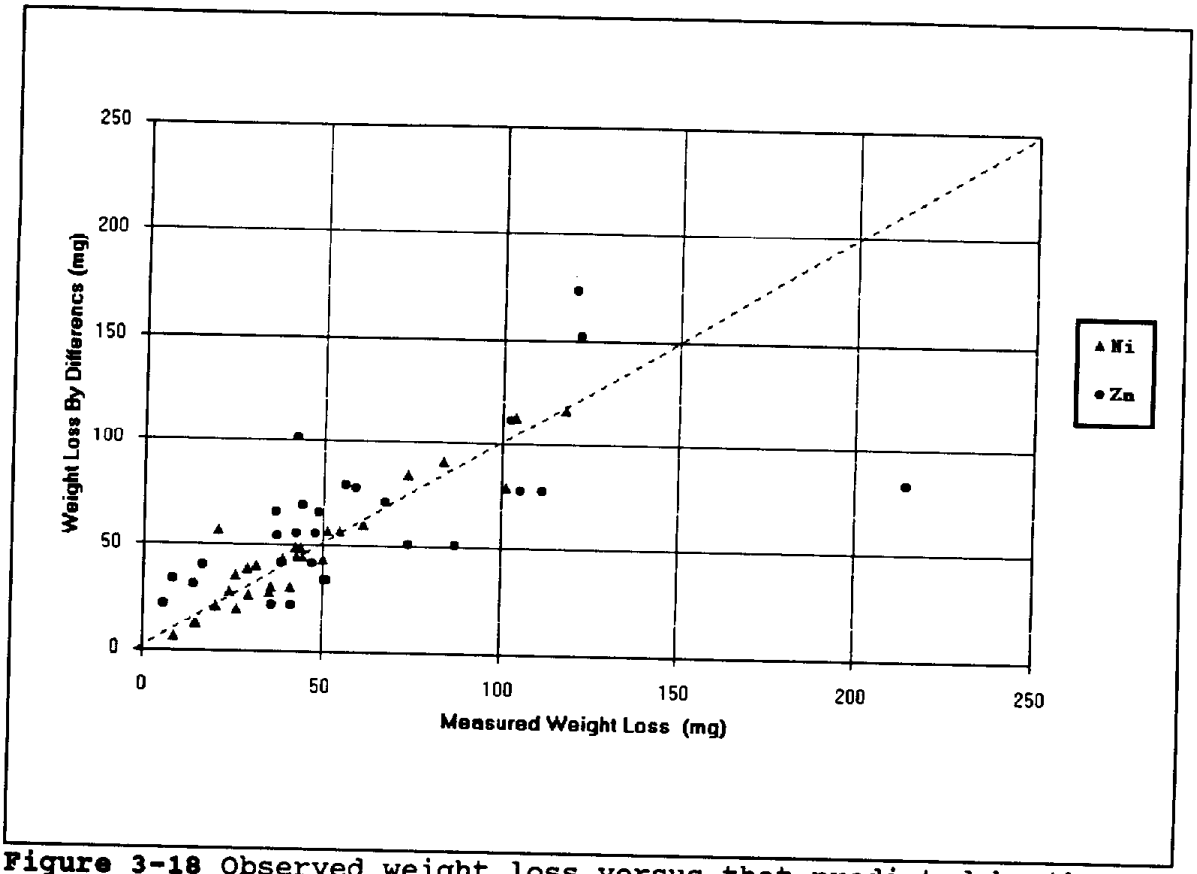

Figure 3-18 Observed weight loss versus that predicted by the difference of two periods.

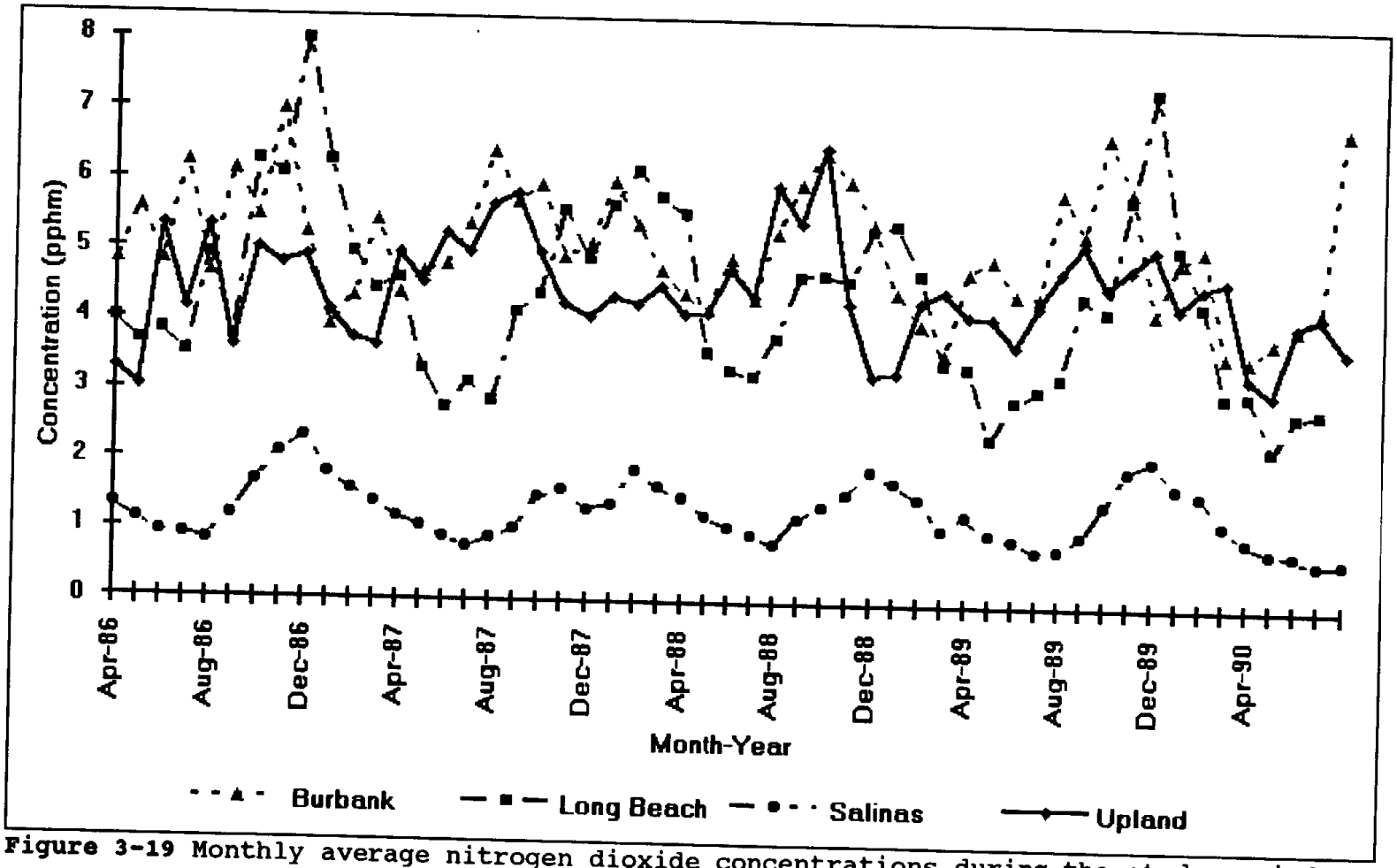

Figure 3-19 Monthly average nitrogen dioxide concentrations during the study period.

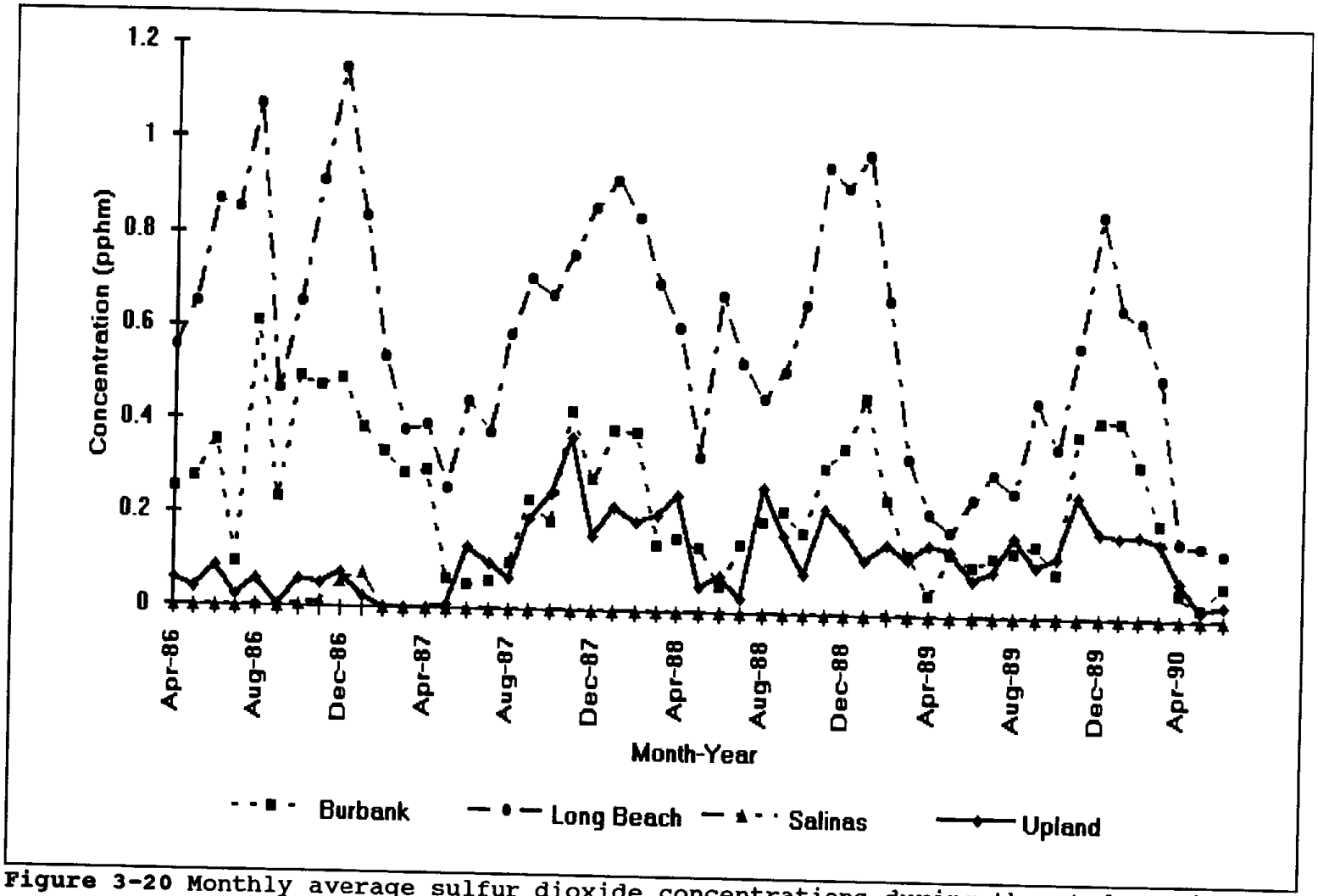

Figure 3-20 Monthly average sulfur dioxide concentrations during the study period.

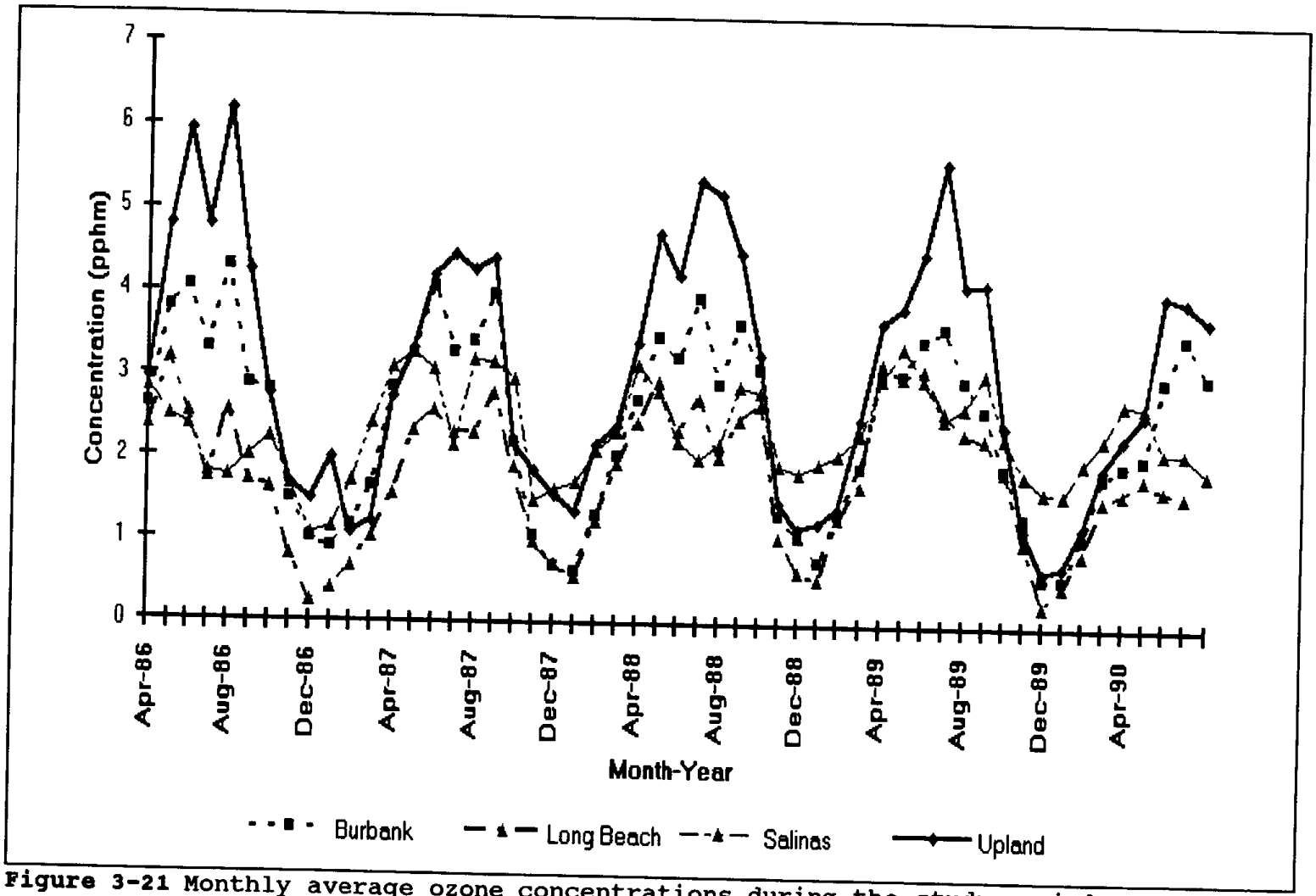

Figure 3-21 Monthly average ozone concentrations during the study period.

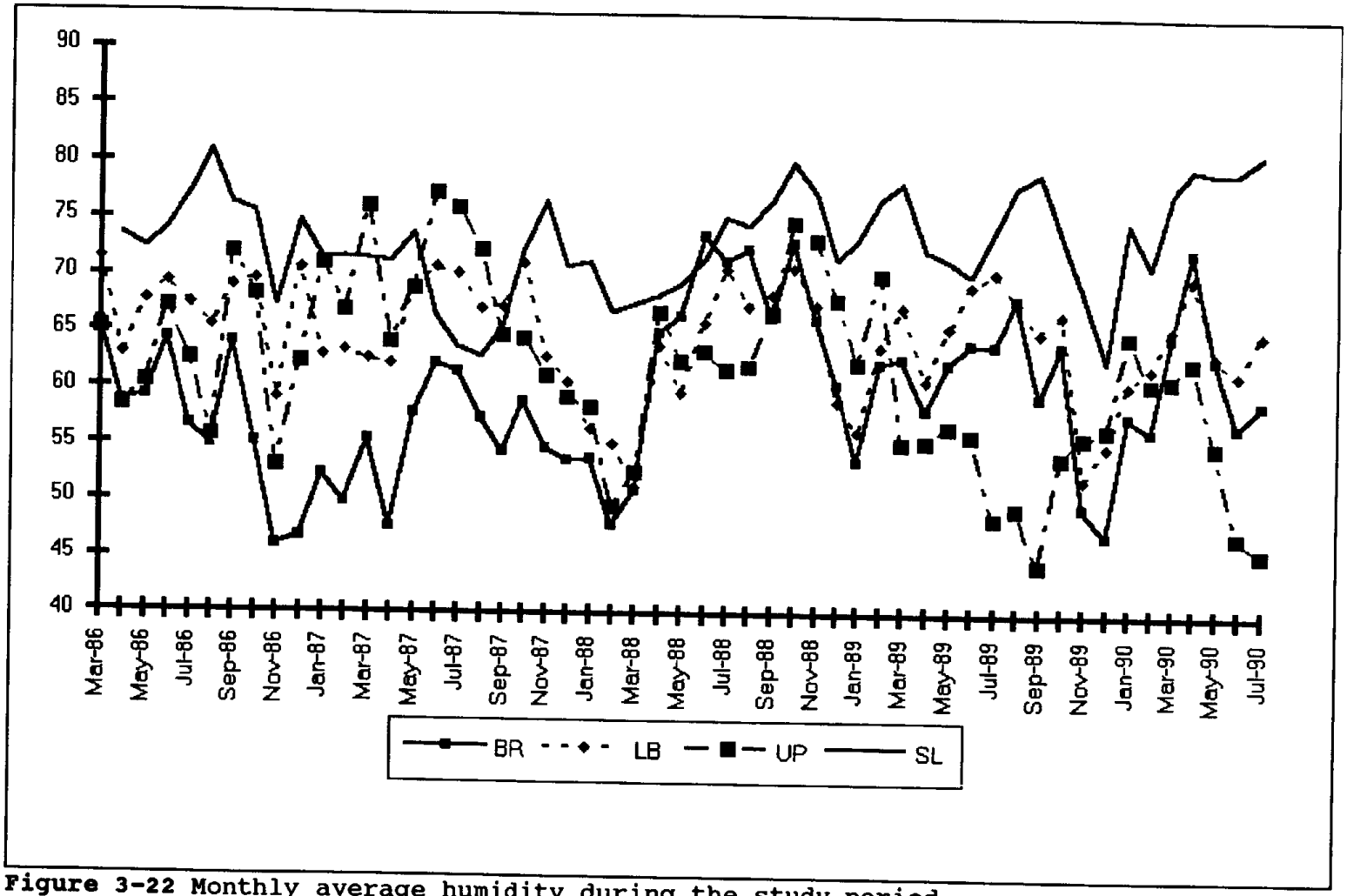

Figure 3-22 Monthly average humidity during the study period.

4 Multivariate Analysis

Correlation analysis, Principal Component Analysis (PCA)(6), and multivariate regression analysis were applied to uncover any relationships between corrosion rates and air quality and meteorological variables. Only the results of the multivariate regression analysis are presented here. PCA was carried out on all the variables, as well as on subsets of weight loss, air quality, and meteorological variables. The component scores of the weight loss components were regressed against the scores of the air quality and meteorological components. However, none of these procedures uncovered any significant relationships that were not better shown by multiple regression. The variables included in the study are given in Table 4-1.

4.1 Correlation Analysis

One means of getting a quick overview of the interdependencies in a data set is the product moment correlation matrix. Table 4-2 contains the correlation matrix of pairwise correlations of the corrosion rate and aerometric variables. Except for the variable Fsmog, most the variables in the Table are self-explanatory. Fsmog is defined as the fraction of the exposure period that occurred during the smog season of May through October. The results of the previous analysis (1) had shown that all or most of the damage may be occurring in these months. This variable

was designed to test that observation.

The correlations are interpreted according to the following guidelines. First, correlations near zero imply that the two variables have no relationship within the data set. Correlations near +1 imply that the two variables vary up and down in unison, while a -1 correlation implies that one variable always increases when the other decreases and vice versa. Of course, most the correlations in a set of variables will not fall into either of these categories. Indeed, because of the common effects of meteorology on pollutant concentrations, most pollutants will almost always be moderately correlated with each other. As an aid to discussion, a level of ±0.5 has been chosen as an indicator of possible significant correlation and values greater than this have been printed in bold in the Table; however,this does not imply a statistical test of significance.

The highest correlation in the Table is 0.88 between H-C paint and nylon damage rates. Examination of the Table shows that neither of these two variables is even moderately correlated with any other variable; thus making physical interpretation of their relationship difficult. In fact, since there were only 52 nylon damage rates, the correlations based on this small a data set are subject to distortion by random errors. Thus, the high correlation between nylon and H-C paint damage rates may not be as significant as it appears. Another possibility is that the

major cause of damage of both materials is ultraviolet light. The next highest correlation between corrosion rates for two materials is Ni and Zn at level of 0.45. This is not a very high correlation and may or may not be significant since it is based on only 64 data points.

Some relationships between corrosion rates and air quality and meteorological variables can be deduced from Table 4-2. The corrosion rate for Zn is correlated highly only with Fsmog and T60-T80 and not at all correlated with precursor acid gases SO_2 and NO_2. Ni corrosion rate, on the other hand, is correlated only with concentrations of these two gases, while damage to the two types of paint is not well correlated with any of the meteorological, seasonal, or air quality variables. Correlations among the air quality and meteorological variables are discussed in the following.

Concentrations of acid gases SO_2 and NO_2 are highly correlated with each other, as expected, because of the forcing effects of meteorology which controls the ability of the atmosphere to disperse pollutants. An unusually high negative correlation in the Table that needs explanation is that of NO_2 with T60. This is almost certainly an artifact of the selection of the study sites. The high values of T60 at Salinas are accompanied by very low values of NO_2, while the NO_2 levels at all the Southern California sites are very much higher. Thus, the highest values

of T60 (at Salinas) occur only with very low values of NO_2, which leads to the large negative correlation. If Salinas were discounted, there would be no correlation of these two variables.

Finally, Fsmog and O_3 are correlated, but only at the 0.519 level, which is not as high as one might expect since the period from May to October is often called the smog season. Actually, the correlation at each individual site is much better than all the sites taken together because the relationship of Fsmog and O_3 seems to be different at each site.

4.2 Regression Analysis

4.2.1 Introduction

The goal of the regression analysis was to calculate physically meaningful equations relating corrosion rates to air quality and meteorological variables. Many equally plausible regression equations can be derived from the data for the corrosion rate of a material. The success of a regression is judged by how many explanatory variables are used, how well the equation explains the observed corrosion rates, and whether the equation makes sense in terms of known physical and chemical processes. Ideally, the regression analysis would result in universal damage functions which could be applied anywhere in California.

The method applied in this study was to simply perform all possible regressions using the best regression command of the MINITAB statistical software (7). From the set of all possible regressions it is usually a simple matter to identify one or two sets of variables which are optimum in the sense of explaining the maximum amount of variability with the minimum number of variables. Once one or two sets of variables were selected for each material, a detailed multiple regression was performed. This included several regression diagnostics that test for the existence of poorly fitted points or points which are very influential in determining the regression coefficients. The results for each material are discussed below.

4.2.2 Ozone As an Indicator for Nitric Acid

Before discussing the outcome of the regression analysis, the special challenges presented by this particular data set must be considered. The major limitation of the data is a lack of measurements of all the important acidic species in the atmosphere. This is particularly true of HNO_3 since it seems to play a major role in corrosion in California (1). This limitation is addressed in the following analysis by using ozone as an indicator for HNO_3 because both are products of photochemical reactions in the atmosphere. HNO_3, both vapor and liquid phase, in the atmosphere is formed primarily by gas phase photochemical reactions (8); thus, it is reasonable to expect

that O_3, which is the major product of these photochemical reactions, will be related to HNO_3.

Using a variable such as ozone in the analysis complicates both the interpretation and the mechanics of doing the regressions. The relationship between ozone concentrations and HNO_3 will, in general, vary from site-to-site, which implies that the relationship between corrosion rate and ozone will also differ from site-to-site. Figure 4-1 shows that this is the case for Zn corrosion rate at two of the study sites, Long Beach and Upland. Figure 4-1 shows that at each site there is a strong linear relationship between corrosion rate and ozone concentration (Burbank and Salinas also have linear relationships but are not shown in order to keep the Figure readable). However, the slope of the line is quite different for the two sites. For this reason, a regression of Zn corrosion rate as a function of ozone concentration using data from all sites would not show the strong relationship which actually exists.

The above analysis would seem to call for restricting the regression analysis to data from one site at a time. Unfortunately, site-by-site analysis is not a good alternative for two reasons. For one, each site has at most 16 corrosion rates for each material, and this is a very small number on which to base a statistical analysis. For another, by restricting the regression to one site the regression will be valid only for the

limited range of conditions at that site; whereas, if data from all sites are included, the regression will be valid over a much larger range of conditions. The solution to this problem is presented in the next section.

4.2.3 Site Indicator Variables

Indicator variables provide a statistical convention for addressing the differences between sites in a regression. An indicator variable for Burbank ozone is defined, for example, as:

$$BRO_3 = \begin{cases} O_3 value, & \text{if the data is for Burbank,} \\ 0, & \text{otherwise} \end{cases} . \qquad (3)$$

This use of indicator variables for the various sites allows for the possibility that the relationship between O_3 and corrosion rate may be different at different sites. In the next section, this concept is applied to Zn corrosion rate.

4.2.4 Zinc (Galvanized Steel)

Without using indicator variables, the best regression equation of Zn corrosion rate versus all other variables included only Fsmog and T60-T80, which is not surprising considering these were the only variables highly correlated with Zn weight loss rate. The equation and some of the statistical details are given in part A of Table 4-3. This regression equation explains over half of the variability in the data with just two variables.

Part B of Table 4-3 gives another regression equation for Zn corrosion rate using ozone site indicator variables. As measured by R^2, this equation is better at predicting Zn corrosion rate than that in Part A of the Table. The rather high R^2 of this equation is shown graphically in Figure 4-2, which shows the good relationship between the observed Zn corrosion rate and that predicted by the equation in Part B of the Table.

4.2.5 Nickel

The best regression equation for Ni corrosion rate is given in Table 4-3. The equation has 5 indicator variables: ozone from Burbank and Upland and T60 (the fraction of time the relativity was less than 60%) from Long Beach, Salinas, and Upland. Essentially, this equation says that Ni corrosion rate is best predicted by ozone alone at Burbank and Upland, by T60 alone at Long Beach and Salinas, and by ozone and T60 at Upland. As the case with Zn, ozone is presumably a surrogate for photochemically produced acids, primarily HNO_3.

The predictive power of the Ni regression is very great as indicated by the very high R^2 and the close agreement between predicted and observed weight loss rate as shown in Figure 4-3.

4.2.6 High and Low Carbonate Paint

None of the regressions of the corrosion rates of the paints explained more than 18% of the variability of corrosion rate, and most explained less than 10%. Although some of these equations are statistically significant, such poor performance indicates at best, a weak physical link and in any case, the equations have too little predictive power to be useful predictors of damage to painted surfaces. Thus, regression equations for paint are not given.

4.2.7 Aluminum

Al damage functions were developed from a different set of data than those described above since many of the Al exposure periods were not coincident with the other materials exposure. The Al exposure groups are shown in Figure 3-17.

Some indication of the structure of the Al data set can be seen from the correlations in Table 4-5. The best regression of Al weight loss rate is given in Table 4-6.

4.2.8 Nylon Fabric

The best regression of nylon fabric damage had an R^2 of only 33.9% and included the variables SO_2 and Fsmog. Examination of the plots of nylon damage rate against these variables indicated little or no apparent relationship. Although nylon is known to

be attacked by HNO_3, there was no relationship between nylon damage rate and the HNO_3 surrogate O_3. Perhaps as in the case with the paints, the primary cause of damage was ultraviolet light.

4.3 Discussion of the Regression Analysis Results

As with any statistically derived relationships, the equations for weight loss presented above are valid only over the range of variables used to develop the equations. Table 4-7 gives the maximum and minimum values of some of the relevant variables for each site for the data set used to calculate the Zn and Ni regression equations. Using the values in Table 4-7, Table 4-8 gives the minimum and maximum corrosion rates for each site for Zn, Ni, and Al. Generally the highest maxima occur at Long Beach or Burbank. The minima sometimes go below zero but not by more than one standard error. At all sites except Long Beach for Ni, the minima are within one or two standard errors of zero. The statistically significant non-zero minimum for Ni at Long Beach may indicate that some other important influence or pollutant has not been taken into account in the equation. One possibility is SO_2, since Long Beach is the only site relatively high in this pollutant.

As shown in Section 4.2.2, ozone's role as a surrogate in the equations for HNO_3 is site-specific, Thus, the regression

equations presented above are site-specific and cannot be applied throughout California to estimate the cost of materials damage due to acid deposition.

4.4 Tables

Table 4-1. Variables Included In the Multivariate Analysis

Variable Type	Variable
Corrosion Rate	Zn, Ni, Al, High and Low Carbonate Paints, Nylon Fabric
Air Quality	CO, SO_2, NO_2, O_3
Meteorological and Seasonal	T60*, T70, T80, T90, T60-T80, Fsmog

* TXX is the fraction of time that relative humidity was greater than XX %. Fsmog is the fraction of the exposure period between May and October.

Table 4-2 Correlations of Corrosion Rate, Air Quality, and Meteorological Variables

	Zn	Ni	LC	HC	Nylon	SO_2	NO_2	O_3	T60	T60-T80
Ni	0.446									
LC	0.182	0.242								
HC	0.109	0.275	0.234							
NY	0.180	0.442	0.405	**0.878**						
SO_2	0.135	**0.621**	0.195	0.301	**0.574**					
NO_2	-0.230	**0.564**	0.093	0.245	0.344	**0.622**				
O_3	0.187	0.198	-0.017	-0.139	-0.140	-0.446	0.001			
T60	0.364	-0.245	-0.053	-0.148	0.058	-0.092	**-0.706**	-0.277		
T60-T80	**0.689**	0.190	0.055	0.142	0.253	0.274	-0.369	-0.25	**0.515**	
Fsmog	**0.500**	0.376	0.258	0.026	0.158	-0.058	-0.132	**0.519**	0.200	.311

Note: correlations of NY are based on 52 data points while all others have 64, Correlations of Al damage rate are given in Table xx.

Table 4-3. Best Regression Equation of Zinc Weight Loss Rate

A. Without site indicator variables

$Zn = - 0.352 + 0.199\ Fsmog + 1.50\ T60\text{-}T80$

63 cases used 5 cases contain missing values

Predictor	Coef	Stdev	t-ratio	p
Constant	-0.35243	0.07007	-5.03	0.000
Fsmog	0.19856	0.05768	3.44	0.001
T60-T80	1.4971	0.2292	6.53	0.000

s = 0.08722 R-sq = 56.2% R-sq(adj) = 54.7%

The units are: Zn corrosion rate, mg/day; O_3, pphm; T60-T80 and Fsmog dimensionless in the range [0,1];

B. With site indicator variables

$Zn = - 0.455 + 1.37\ T60\text{-}T80 + 0.100\ BRO_3 + 0.143\ LBO_3$
$0.106\ SLO_3 + 0.0760\ UPO_3$

63 cases used 5 cases contain missing values

Predictor	Coef	Stdev	t-ratio	p
Constant	-0.45535	0.09168	-4.97	0.000
T60-T80	1.3676	0.3428	3.99	0.000
BRO_3	0.10005	0.02139	4.68	0.000
LBO_3	0.14346	0.03534	4.06	0.000
SLO_3	0.10585	0.02770	3.82	0.000
UPO_3	0.07599	0.01466	5.18	0.000

s = 0.07999 R-sq = 65.0% R-sq(adj) = 61.9%

XXO_3 is equal to the average O_3 at site XX for data points from site XX and is equal to zero for data from other sites.

Table 4-4 Best Regression of Nickel Corrosion Rate

$Ni = -0.146 + 0.147\ BRO_3 + 0.0416\ UPO_3 + 0.517\ LBT60 + 0.276\ SLT60 + 0.257\ UPT60$

63 cases used 5 cases contain missing values

Predictor	Coef	Stdev	t-ratio	p
Constant	-0.14599	0.03214	-4.54	0.000
BRO_3	0.14663	0.01249	11.74	0.000
UPO_3	0.04156	0.00867	4.79	0.000
LBT60	0.51707	0.04650	11.12	0.000
SLT60	0.27586	0.04230	6.52	0.000
UPT60	0.25671	0.07344	3.50	0.001

s = 0.03242 R-sq = 87.3% R-sq(adj) = 86.2%

Ni corrosion rate is in mg/day. O_3 variables are in pphm, and T60 is a fraction between 0 and 1.

Table 4-5 Correlations of the Aluminum Data Set

	Al	SO_2	NO_2	O_3	T60	T60-T80
SO_2	0.303					
NO_2	-0.055	0.612				
O_3	0.049	-0.587	-0.152			
T60	0.381	-0.130	-0.768	0.038		
T60-T80	0.679	0.028	-0.437	0.013	0.547	
Fsmog	0.563	-0.149	-0.110	0.608	0.372	0.523

Table 4-6 Best Regression of Aluminum Weight Loss Rate

Al = - 0.274 + 0.780 T60-T80 + 0.0577 BRO_3 + 0.0873 LBO_3 + 0.0396 SLO_3 + 0.0384 UPO_3

Predictor	Coef	Stdev	t-ratio	p
Constant	-0.27434	0.06709	-4.09	0.000
T60-T80	0.7801	0.2442	3.19	0.003
BRO_3	0.05769	0.02517	2.29	0.029
LBO_3	0.08730	0.03405	2.56	0.016
SLO_3	0.03958	0.02619	1.51	0.141
UPO_3	0.03837	0.01820	2.11	0.044

s = 0.04758 R-sq = 62.5% R-sq(adj) = 56.0%

Analysis of Variance

SOURCE	DF	SS	MS	F	p
Regression	5	0.109244	0.021849	9.65	0.000
Error	29	0.065655	0.002264		
Total	34	0.174898			

The Al loss rate is in mg/day. O_3 variables are in pphm, and T60-T80 is a fraction between 0 and 1.

Table 4-7 Range of Variables Used To Develop Zinc and Nickel Regression Equations

	SO2 MAXIMUM	NO2 MAXIMUM	O3 MAXIMUM	T60 MAXIMUM	Fsmog MAXIMUM	T60-T80 MAXIMUM
BR	0.515	6.30	3.58	0.576	1.00	0.435
LB	0.926	6.89	2.62	0.775	1.00	0.395
SL	0.053	1.99	2.81	0.892	1.00	0.442
UP	0.226	5.25	5.16	0.676	1.00	0.322
ALL	0.926	6.89	5.16	0.892	1.00	0.442

	SO2 MINIMUM	NO2 MINIMUM	O3 MINIMUM	T60 MINIMUM	Fsmog MINIMUM	T60-T80 MINIMUM
BR	0.189	4.74	1.35	0.334	0.129	0.240
LB	0.434	3.97	0.93	0.609	0.142	0.297
SL	0.000	0.997	1.54	0.694	0.000	0.280
UP	0.026	3.68	1.85	0.457	0.130	0.211
ALL	0.000	0.997	0.93	0.334	0.000	0.211

The units of the gases are pphm, all the other variables are dimensionless.

Table 4-8 Corrosion Rates (μm/yr) Calculated by Regression Equations

	Zn	Ni	Al
Maximum Corrosion Rate			
BR	0.822	0.503	1.19
LB	0.759	0.338	1.15
SL	0.741	0.132	0.79
UP	0.625	0.320	0.76
Minimum Corrosion Rate			
BR	0.0148	0.06885	-0.039
LB	0.1386	0.22376	0.169
SL	0.1518	0.05958	0.008
UP	-0.0429	0.06355	-0.167
Standard error*	0.130	0.042	0.197

*Applies to both maximum and minimum estimated corrosion rates.

4.5 Figures

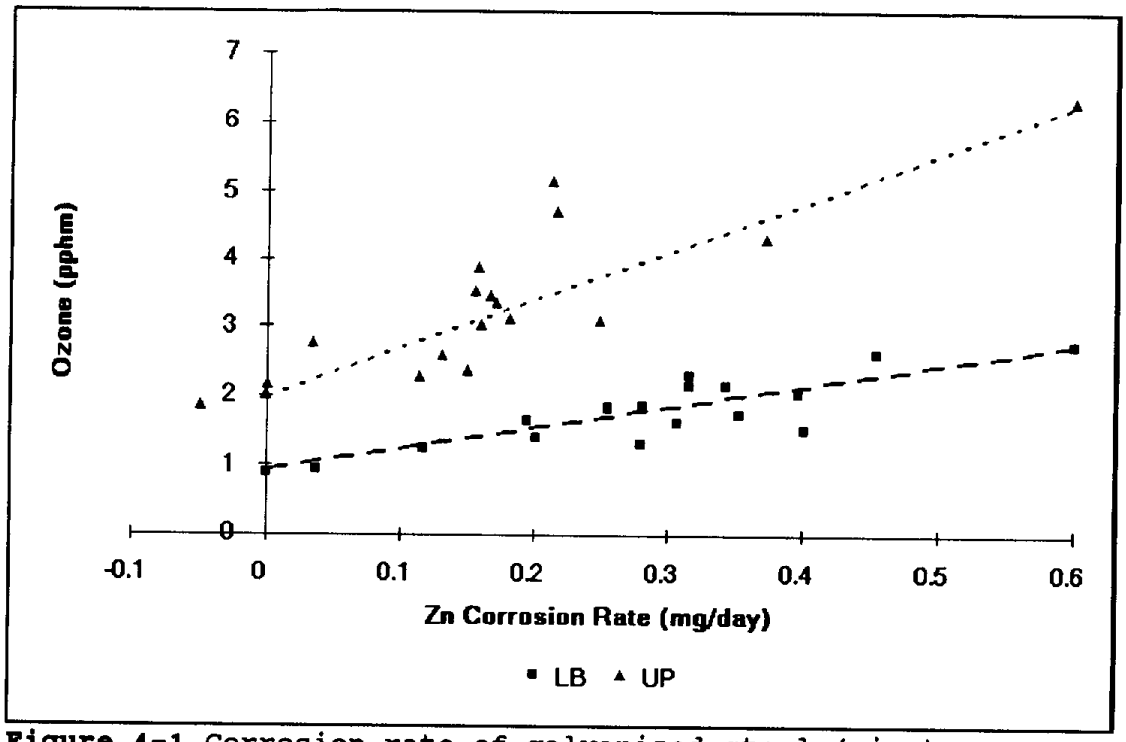

Figure 4-1 Corrosion rate of galvanized steel (zinc) versus average ozone concentration at Upland and Long Beach.

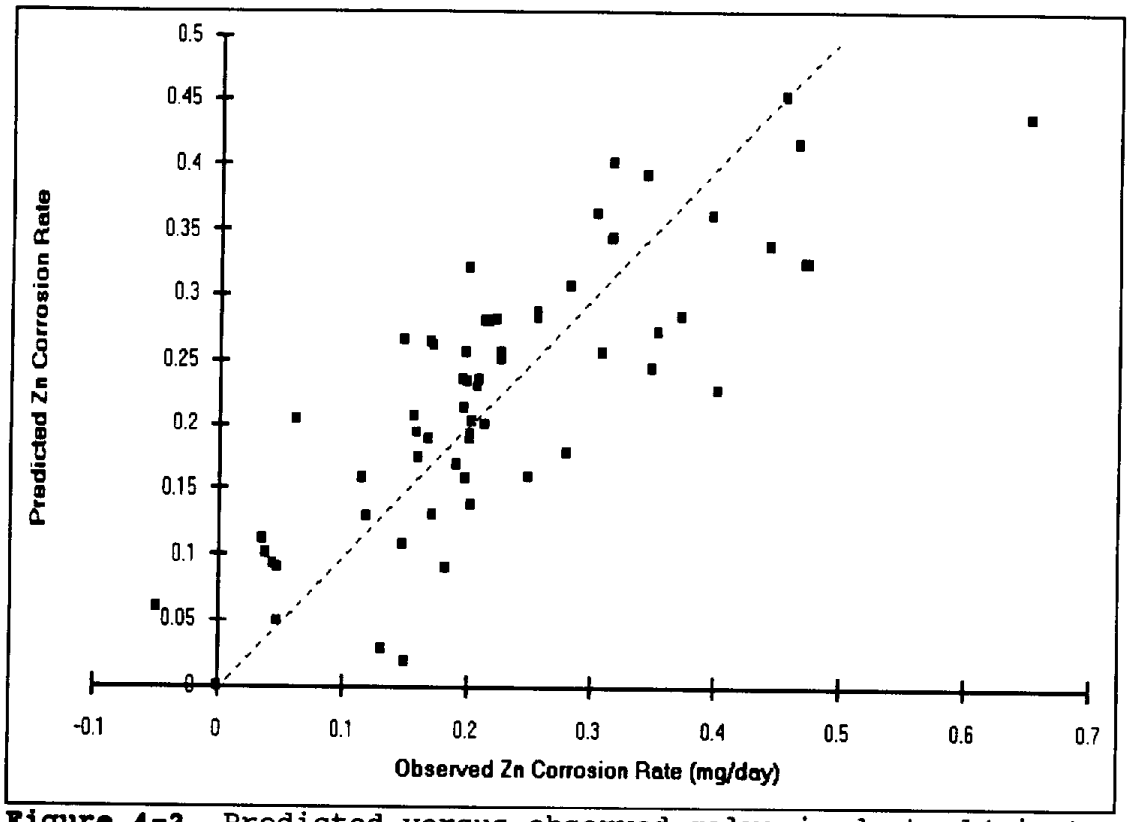

Figure 4-2. Predicted versus observed galvanized steel(zinc) corrosion rates.

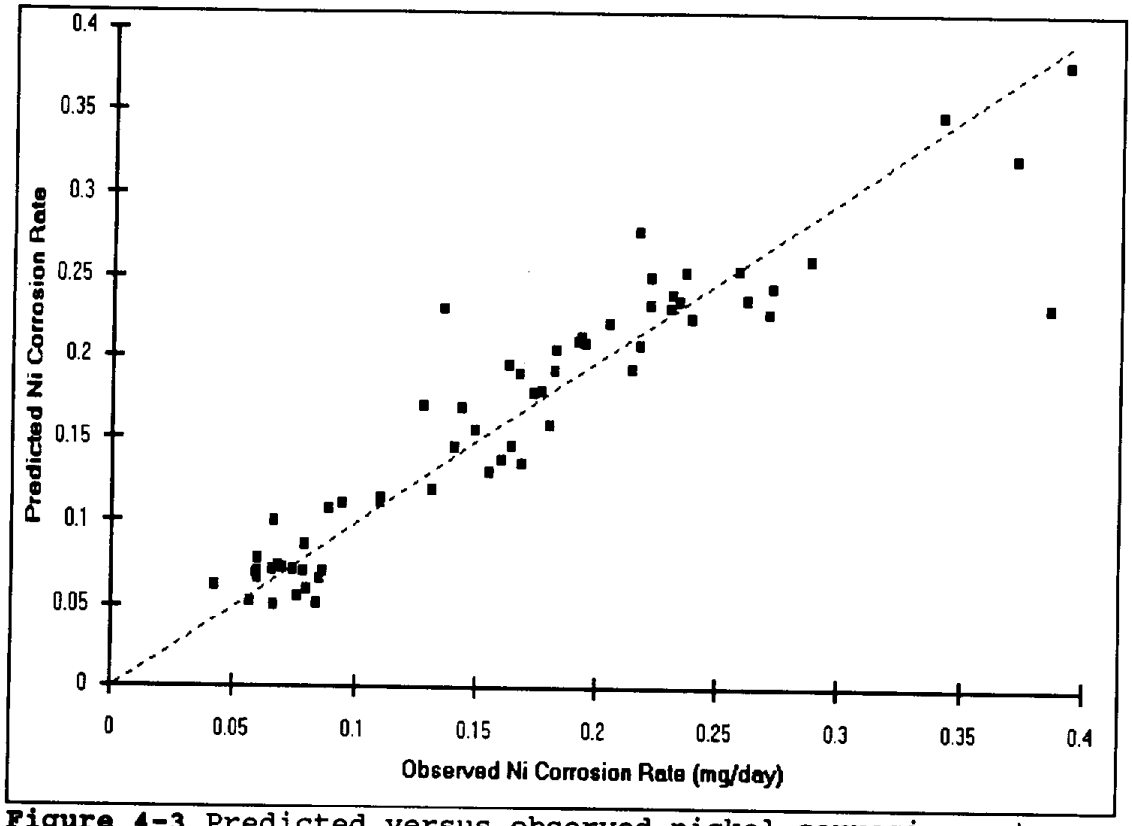

Figure 4-3 Predicted versus observed nickel corrosion rates.

5 Summary and Conclusions

Exposure tests were carried out between March 1986 and August 1990 at three test sites in Southern California (Burbank, Long Beach and Upland) and at a background site in Central California (Salinas). The materials investigated in this study were chosen based on their economic importance and included galvanized steel, nickel, aluminum, two types of flat latex exterior house paint, nylon fabric, polyethylene and concrete. Atmospheric data were provided by CARB's air monitoring network at each test site. Relative humidity data were obtained from local airports.

The major objectives of this phase of the project were to determine corrosion damage to the selected materials and to relate damage data to concentrations of atmospheric pollutants and meteorological variables, especially relative humidity.

Corrosion rates were very low for galvanized steel and nickel at all four test sites. Using galvanized steel, which has been employed as a "standard material" in most atmospheric corrosion tests, a relative measure of the corrosivity of the four test sites can be estimated. The average corrosion rate at the three sites in Southern California was 7.0 mg/ m^2-day (2.56 g/m^2-year) or 0.36 μm/year, which is a very low value usually observed only at "clean" sites (4). For comparison, corrosion rates for pure zinc determined in the program ISO CORRAG sponsored by the

International Standards Organization (ISO) ranged from 1.6 to 2.0 μm/year for test sites at Kure Beach, North Carolina, Newark-Kearny, New Jersey, and Point Reyes, California. At a test site at USC an average annual corrosion rate over a four year period of 1.15 μm/year was determined between March 1987 and March 1991 (9).

For nickel, average corrosion rates range between 0.09 μm/year at Salinas and 0.28 μm/year at Burbank and Long Beach. Nickel is not part of the ISO CORRAG study, therefore no comparison with the other test sites in the USA could be made. Average corrosion rates over a ten year period for nickel have been reported as 3.25 μm/year in New York City (urban-industrial), 0.10 μm/year in La Jolla, California (marine) and 0.15 μm/year in State College, Pennsylvania (rural) (10).

For Al, for which fewer data points were available, an average corrosion rate of 0.42 μm/year was determined in this study. This result agrees well with the average corrosion rates between 0.45 and 0.61 μm/year measured at USC in the ISO CORRAG study (9). It is interesting to note that corrosion rates determined at the other three test sites in the USA were lower (0.16 - 0.29 μm/year) than those measured at the test sites in the South Coast Air Basin. The atmospheric pollutants which cause higher corrosion rates for Al at the test sites in Southern California do not appear to accelerate corrosion rates of zinc or galvanized

steel. Since Al is susceptible to HNO_3 and to localized attack by chlorides, it is possible that HNO_3 formed by photochemical oxidation of NO_x and chlorides transported from the ocean produce these high corrosion rates. The effect of chlorides is likely at Long Beach (0.55 μm/year), which is close to the ocean and has the highest Al corrosion rates (Table 3-3). On the other hand, the lowest corrosion rates were observed at Upland (0.20 μm/year), which is an arid, inland site furthest from the ocean. According to Kucera and Mattson (4), mean corrosion rates determined from weight loss data for Al in marine atmospheres are between 0.4 and 0.6 μm/year, which is in the range determined in this study. The high corrosion rates for Al relative to the low corrosion rates for other materials in this study are quite unusual and were unexpected. Since Al is an increasingly important structural material, further research into the causes of the high Al corrosion rate in Southern California is recommended. Emphasis should be on measurements of HNO_3 and chlorides at the test sites, chemical analysis of the corrosion products and determination of the morphology of the corrosive attack by microscopic observation.

Closer analysis of the time dependence of corrosion rates for galvanized steel, nickel and aluminum reveals unusual trends insofar as corrosion rates are higher in the summer months than in the winter months. In most published exposure studies, the opposite behavior has been observed with corrosion rates being

higher in the winter when SO_2 concentrations are higher(4). In fact, a recent review of damage functions for zinc and galvanized steel has shown that corrosion rates have been correlated only with the SO_2 concentration or with SO_2 concentration and RH or time-of-wetness (4). Clearly, such damage functions cannot be used to explain the time dependence of the corrosion rate data determined at the test sites used in this project where SO_2 concentrations are very low (Fig. 3-20). It is very likely that the higher corrosion rates observed in the summer are due to increased levels of photochemically formed acidic gases - HNO_3 vapor and perhaps also HCl vapor and organic acids. However, valid data for these pollutants were not available during the period of the materials exposures. In the winter, corrosion rates for galvanized steel and nickel were very low, which could be due to the low SO_2 concentration, the cleaning effect of rain and other factors which could not be determined in this study.

Multiple regression analysis of the relationships between corrosion rates and aerometric variables found that the damage to nickel, zinc, and aluminum could be explained by O_3 and humidity related variables. Presumably, O_3 is an indicator for photochemically produced acid vapors, since it does not attack any of the materials used in this study (1). However, the relationship between O_3 and corrosion rates was site-specific and, thus the results cannot be extended to estimate damage at other locations in California. In particular, the regression equations developed

in this study cannot and should not be used to estimate the cost of materials damage. For the two paints and nylon fabric, a regression equation could not be found which explained the observed corrosion rates.

6 References

1. Vijayakumar, R., F. Mansfeld, and R. Henry. "Investigation of the Effects of Acid Deposition On Materials, Final Report." CARB Contract Nos. A4-110-32 and A5-137-32, October, 1989.

2. Mansfeld, F. R. Henry, and R. Vijayakumar. "The Effects of Acid Fog and Dew on Materials, Final Report." CARB Contract No. A4-138-32, October, 1989.

3. Horie, Y. A., A. Shrope, R. Ellefsen. "Development of an Inventory of Materials Potentially Sensitive to Ambient Atmospheric Acidity in the South Coast Air Basin, Final Report." CARB Contract No. A6-079-32, March, 1989.

4. Kucera V. and E. Mattson. "Atmospheric Corrosion," in Corrosion Mechanisms, F. Mansfeld, editor, Marcel Dekker, 1987.

5. Watson, J. G., J. C. Chow, R. T. Egami, J. L. Bowen, C. A. Frazier, A. W. Gertler, D. H. Lowenthal, and K. K. Fung. "Measurements of Dry Deposition Parameters for the California Acid Deposition Monitoring Program, Final Report." CARB Contract No. A6-076-32, June, 1991.

6. Henry R. C. and G. M. Hidy. "Multivariate Analysis of Particulate Sulfate and Other Air Quality Variables by Principle

Components, Part I, Annual Data from Los Angeles and New York." Atmospheric Environment 13:1581-1596, 1979.

7. Minitab Statistical Software, Version 6 for the IBM PC. Minitab, Inc., 3081 Enterprise Drive, State College, PA 16801.

8. Seinfeld, J. H. Atmospheric Chemistry and Physics of Air Pollution, John Wiley & Sons, Chapter 4, 1986.

9. Dean, S. W. "ISO CORRAG Collaborative Exposure Program, Fourth Exposure Report on the USA Program," Air Products and Chemicals, Inc., December, 1992.

10. Uhlig H. H. and R. W. Revie. Corrosion and Corrosion Control, third edition. John Wiley & Sons, 1985.